Magma-Metal Series Classification of Mineralization in the Vicinity of Yucca Mountain, Nevada

Jan C. Rasmussen*
Jan Rasmussen Consulting, P.O. Box 36971, Tucson, AZ 85740

Stanley B. Keith*
MagmaChem Exploration, Inc., P. O. Box 672, Sonoita, AZ 85637

ABSTRACT

This paper applies the magma-metal series classification developed by Keith and others (1991) and Keith and Swan (1996) to mineralization of southwestern Nevada, including the Nevada Test Site (NTS), Yucca Mountain, and surrounding areas. A new Ultra-Deep Hydrocarbon (UDH) hydrothermal oil model (Keith and others, 2008) also applies to the region. Mineralization was emplaced from mid-Cretaceous to late Miocene time. Mineralization related to the Miocene volcanism at Yucca Mountain proper did not contain sufficient hydrous minerals to suggest there was potential for economic mineralization, in contrast to well mineralized districts around Beatty to the SW.

Cretaceous magmatism and related mineralization in the NTS region includes: 1) the Climax stock (metaluminous alkali-calcic [MAC]) at 102–99 Ma; 2) the Gold Meadows stock (metaluminous calc-alkalic [MCA]) at 93–96 Ma, which can produce copper-molybdenum-silver porphyry systems; 3) peraluminous calcic (PC) tungsten associated with pegmatite dikes (PC2 of Late Cretaceous age); and 4) peraluminous calc-alkalic (PCA3A) gold-quartz veins at 85–72 Ma.

Cretaceous MAC and MCA magmatism reflects flattening subduction between 100 and 90 Ma. The main structures accompanying metaluminous magmatism were east-directed thrust faults (e.g., the Belted Range thrust) that were broadly related to the Sevier orogeny in eastern Nevada and western Utah.

Peraluminous magmatism probably resulted from flat subduction beneath the region between 90 and 72 Ma. Structures related to this flat subduction include west-directed mylonite fabrics in low-angle thrust faults related to peraluminous sills in northern Bare Mountain and south of Beatty, and possibly to the WNW-directed CP thrust east of Yucca Mountain.

Tertiary mineralized systems in the region are metaluminous and include: 1) calc-alkalic [MCA] gold mineralization at 13.8–14.9 Ma; 2) alkali-calcic [MAC] base-metal mineralization of the central arc at 12.8–11.2 Ma; 3) quartz-alkalic [MQA] gold mineralization of the late arc at 10 Ma; and 4) nepheline alkalic [MNA] gold-telluride mineralization of the terminal arc at 8 Ma. Increasing alkalinity with decreasing age reflects a rapidly steepening subducting slab beneath the Yucca Mountain area between 15 and 7 Ma.

MCA gold mineralization of the early Miocene arc includes mines on the east flank of Bare Mountain and Paleozoic-hosted mineralization presently deeper than 4800 feet at Yucca Mountain. Examples include Sterling and Mother Lode on the east side of Bare Mountain.

Most of the Miocene igneous rocks in and near the Nevada Test Site are associated with the Southwest Nevada Volcanic Field erupted from 17 to 7 Ma. Most of the volume of volcanic rocks at Yucca Mountain is MAC magma-metal series, commonly associated with lead-zinc-silver-tin mineralization throughout the world. MAC vol-

*E-mail: geoarizona@gmail.com; mcheme@aol.com

canism and associated base-metal mineralization are related to the central part of the magmatic arc. These MAC districts include: 1) silver-base metal mineralization at 12.6–12.8 Ma of the Wahmonie district; 2) hot spring and probable epithermal tin mineralization at 13.5–12.7 Ma in the Beatty Mountain sinter area, Thirsty Canyon—Sleeping Butte area, and West Transvaal district; 3) mercury/fluorite/alunite mineralization at 12.9–11.2 Ma in the northern Bare Mountain area, Mary/Diamond Queen mine, Telluride mine, Southern Calico Hills, western Calico Hills, Claim Canyon mercury anomaly areas, Transvaal East district; and widespread pyritic mineralization in the Tram Ridge Tuff, southwestern Mine Mountain, and 4) northern Yucca Mountain area.

The last major Miocene mineralization in the Yucca Mountain area is associated with quartz alkalic (MQA) magmatism in the trailing portion of the southward-migrating magmatic arc. MQA gold districts include gold-only/adularia mineralization at 10 Ma in the West Bare Mountain, and Bullfrog district (Bullfrog mine, Montgomery-Shoshone mine, Bonanza Mountain area, Original Bullfrog mine, Gold Bar mine, Mayflower-Pioneer area/North Bullfrog), Clarkdale district, and Tolicha district.

The latest metallic mineralization event was the basanitic, nepheline alkaline (MNA) volcanism associated with minor volumes of gold/telluride mineralization. These systems are dated at about 7 Ma in the Beatty area and possibly at the Oasis Mountain gold-telluride system.

Calderas and associated mineralization were probably emplaced in a transpressional regime that affected right slip on the Walker Zone to the north and on the Las Vegas Shear Zone–Stateline-Pahrump fault on the south. These two systems are connected by a north-south trending, dilational jog that includes most of the calderas. This area also includes a N-S trending normal-fault swarm and the north-south trending, Kawich-Greenwater gravity low. Extension in the dilatant jog created most of the room into which calderas and associated hydrothermal activity were emplaced. Minor antithetic tilting on the N-S faults (especially on Bare Mountain) created a gravitational ramp where local gravitational sliding occurred in the Bullfrog Hills tilt domain. Denudational sliding reused pre-existing, low-angle thrust faults that had accompanied Cretaceous magmatism.

Between 7 and 4 Ma, hydrous, iron-poor, metal-bearing magmatism changed to anhydrous, iron-rich, non-metallic magmatism. After 4 Ma, magmatism at Crater Flat contains anhydrous ferromagnesian minerals (such as olivine and pyroxenes), has no epigenetic mineralization, and has strong iron enrichment in typically low-volume felsic differentiates. Basaltic volcanism is associated with Basin and Range, high-angle, normal faults that are in a transtensional regime driven by far-field extension. In contrast, earlier arc-related tectonism was driven by far-field transpression.

The youngest, most widespread hydrothermal activity in the Yucca Mountain area may be associated with hydrothermal oil developed from ultra-deep sources associated with serpentinization in the lower crust. Railroad Valley is the closest system that may be an example of this process. Evidence for this hydrothermal activity includes: basaltic volcanism at Crater Flat; extensive dolomitization in the Paleozoic carbonates beneath the Tertiary rocks; widespread, magnesium-charged, light $\delta^{13}C$ isotopes; and warm (25–35°C) water discharge throughout the Yucca Mountain area. These features are consistent with a UDH, hydrothermal oil system that could underlie Crater Flat beneath a coinciding magnetic high and gravity low.

INTRODUCTION

Applying the magma-metal series classification and stratotectonic approach to the magmatism, geochronology, mineralization, and tectonics of a region is highly effective in assessing the types of ore deposits that may be expected in a region. Because these classes are genetically related to igneous geochemistry and tectonics, they are effective in predicting the types of ore deposits that are likely to occur in a region. More detailed descriptions of the magma-metal series models as applied to the Great Basin have previously been published (Keith and others, 1991; Keith and Swan, 1996) and as applied to the Laramide porphyry copper province in Arizona (Keith and Wilt, 1985, 1986; Keith, 1986). A statistical evaluation of parts of the magma-metal series was presented by Wilt (1993, 1995).

The Yucca Mountain (YM) and Nevada Test Site (NTS) areas have not been available for exploration for about 70 years, yet the areas have been intensively studied. Before the potential radioactive waste repository at Yucca Mountain could be licensed, legislation required that the area and surrounding region be examined for the potential for ore deposits. An evaluation of these areas by the present authors (CRWMS, 1997) assigned magma-metal series model numbers to each mineralized system. The extensive geochemical analyses of mineralized areas conducted by the Nevada Bureau of Mines and Geology (Castor and others, 1999) were used in assigning the systems to a magma-metal series model. Although this discussion primarily concerns YM and NTS, there is considerable commentary on magma-metal series in mineralized districts in the Beatty and Bare Mountain areas and parts of Nellis AFB Range and surrounding regions.

MAGMA-METAL SERIES MODELS IN SOUTHWESTERN NEVADA

Hundreds of mines occur within 300 km of Yucca Mountain. These mines, mining districts, and mineralized areas were classified according to magma-metal series model types (Keith and others, 1991; Keith and Swan, 1996; Wilt, 1993). Approximately 40 geologically distinct mineral systems are recognized within the Nevada Test Site and surrounding regions (Figure 1). Not all mineralized areas within a specific magma-metal series class are economic or have the potential to be economic. The classes are only an indication of which metals are likely to be present.

Ages, alkalinity, and characteristic elements of the mineralized systems in the area are summarized in Table 1. Information on each mineralized area was integrated into the stratotectonic framework provided by Sawyer and others (1994) and the petrochemical cycle concepts of Broxton and others (1986, 1989). A stratigraphic column of the major formations is presented in Figure 2.Very high-quality data from Castor and others (1999) record extremely low concentrations of metallic elements. The data set is dominated by low metal values that are not normally considered anomalous, although meaningful patterns exist within the low-concentration ranges. The following interpretation of mineralization in and near the Nevada Test Site is arranged with the oldest first.

Metallic mineralization ages and districts in southwestern Nevada include:

1. **Mid-Cretaceous (?) base metal (tungsten) mineralization** (Oak Spring district, Johnnie district, northern Calico Hills base metal veins, central Calico Hills brucite alteration, Mine Mountain North, White Rock Springs district;
2. **Mid- to Late Cretaceous peraluminous gold and/or tungsten mineralization** (Lee, Johnnie, Skidoo, Ballarat, and Briggs districts);
3. **Possible Paleogene oil shales associated with deep-seated UDH serpentinite-sourced brines** (Sheep Pass Formation, Elko formation, and rocks of Joshua Hollow(?);
4. **Tertiary (13.8–14.9 Ma) Au (minor As, Hg, Pb, Te, Tl) mineralization** (East flank of Bare Mountain [Sterling mine, Mother Lode mine, Joshua Hollow prospect]);
5. **Tertiary (12.6–12.8 Ma) silver-base metal mineralization** (Wahmonie district);
6. **Tertiary (13.5–12.7 Ma) sinter/adularia/tin mineralization** (Beatty Mountain anomalous sinter area, Thirsty Canyon—Sleeping Butte area, West Transvaal district);
7. **Tertiary (12.9–11.2 Ma) mercury/fluorite/alunite mineralization** (Northern Bare Mountain area, Mary/Diamond Queen mine, Telluride mine, Southern Calico Hills mercury anomaly area, Western Calico Hills mercury anomaly area, Claim Canyon mercury anomaly area, Transvaal East (Buttonhook) district, Tram Ridge mining area [Thompson mine, Silica (Silicon) mine], Southwestern Mine Mountain, Northern Yucca Mountain area);
8. **Tertiary (10 Ma) gold-only/adularia mineralization** (West Bare Mountain, Bullfrog district [Bullfrog mine, Montgomery-Shoshone mine, Bonanza Mountain area, Original Bullfrog mine, Gold Bar mine, Mayflower-Pioneer mine/ North Bullfrog area], Clarkdale district, Tolicha district);
9. **Tertiary (8 Ma) gold/telluride mineralization** (Northern Bare Mountain area, [Daisy mine, Secret Pass deposit], Oasis Mountain area, Central Clarkdale area), and
10. **Tertiary-Quaternary (4–0 Ma) possible potential for hydrothermal hydrocarbon** (Crater Flat and other late Tertiary carbonaceous shales throughout the region, Railroad Valley type, Grant Canyon, Bacon Flat, Pine Valley, Blackburn, and Trap Spring).

CRETACEOUS MAGMATISM AND MINERALIZATION

The oldest recognized mineralization in the region surrounding Yucca Mountain is related to the eastward-migrating, Cretaceous arc system, which was emplaced in southwestern Nevada from 102 to 72 Ma. The Cretaceous magmatism and mineralization (Table 2) can be subdivided into two distinctly different systems: metaluminous at 102–90 Ma, followed by peraluminous at 89–72 Ma. The metaluminous system can also be subdivided into two subsystems: the Climax stock, which is metaluminous alkali-calcic (MAC) at 102–99 Ma, followed by

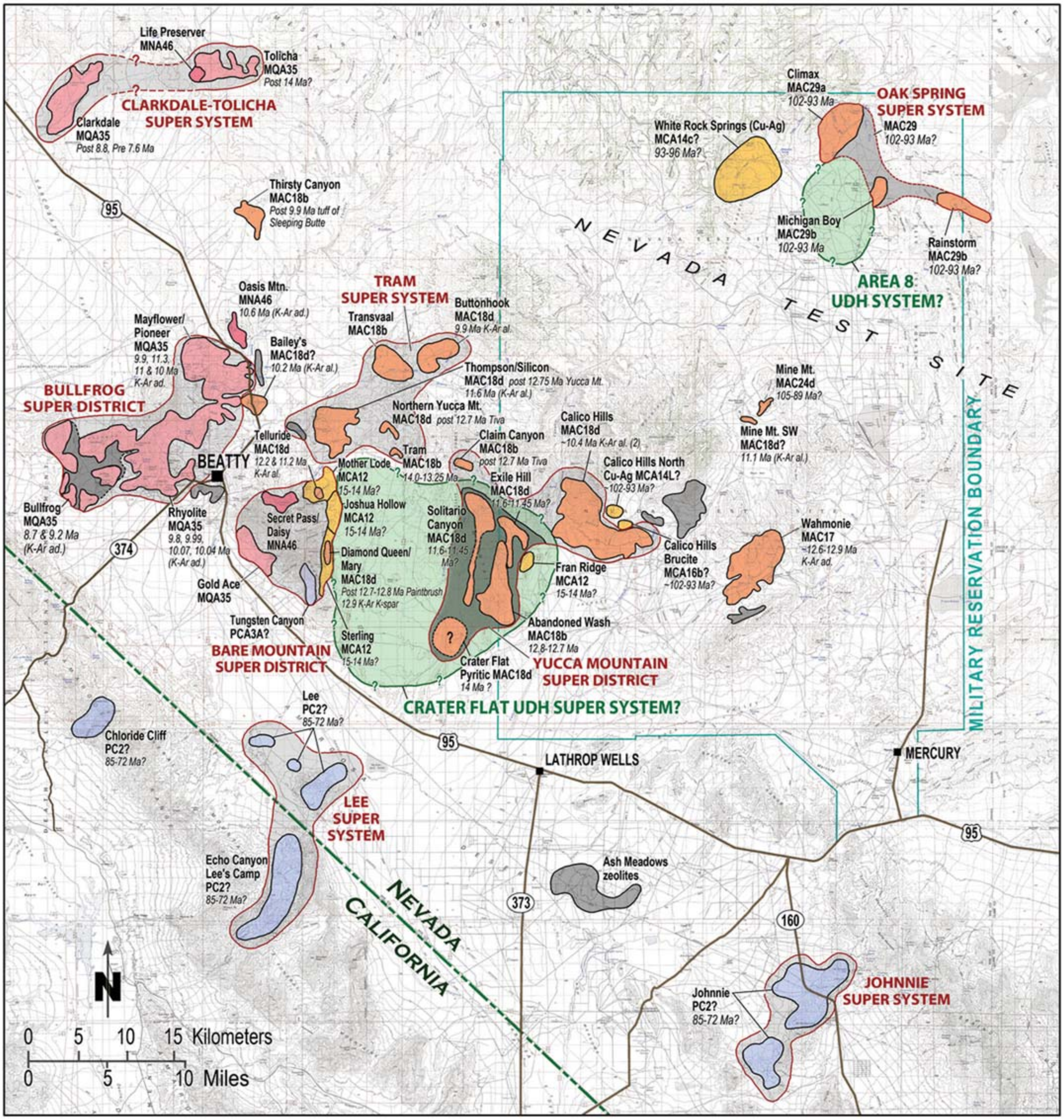

Figure 1. Map of mining districts in and near the Nevada Test Site (yellow is MCA, orange is MAC, pink is MQA, blue is PC, grey outlines the larger area [super system], green is potential UDH areas).

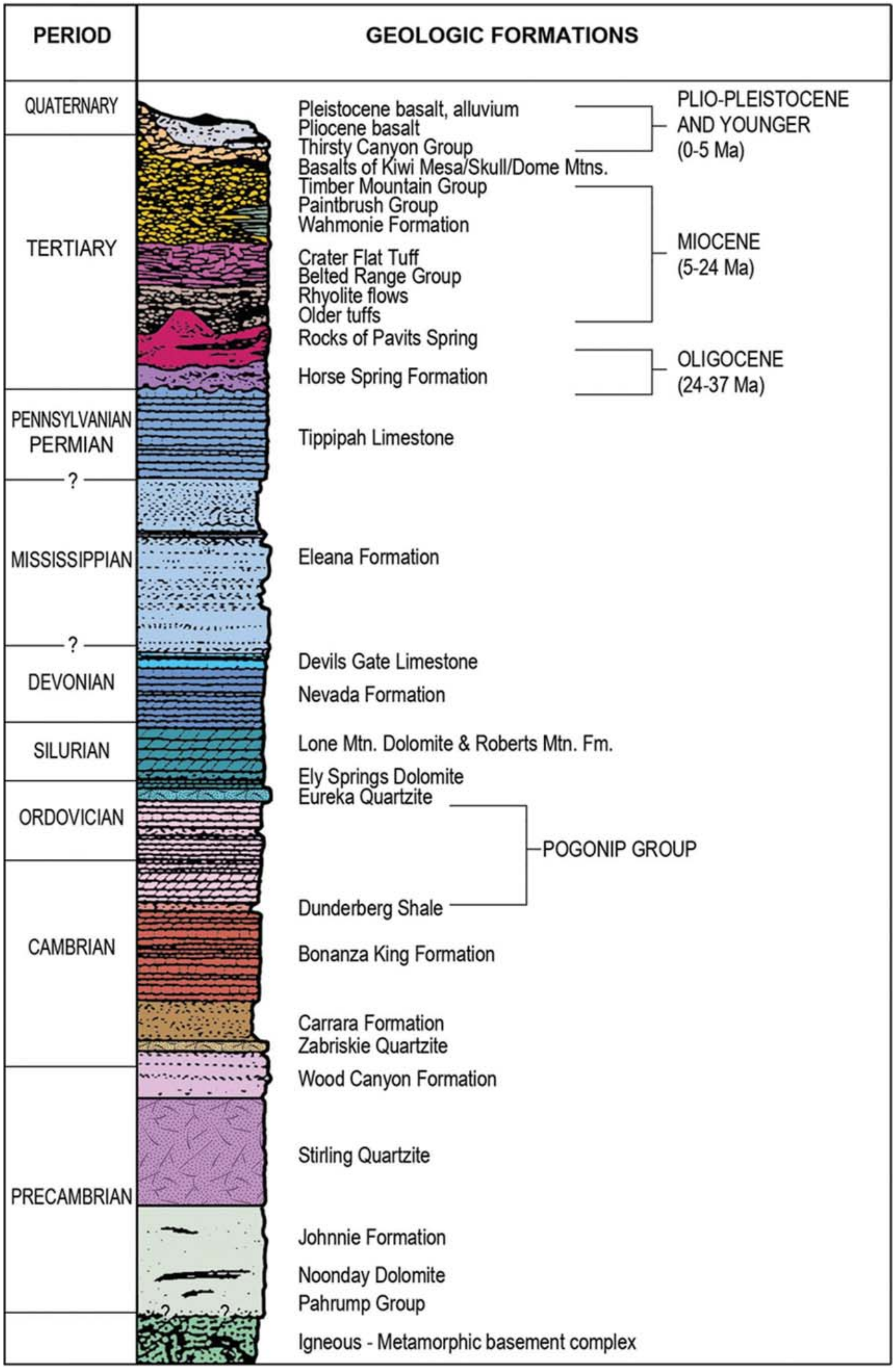

Figure 2. Stratigraphic section for southwestern Nevada (modified from Mattson and others, 1994; Sawyer and others, 1994).

Table 1. GENERAL MAGMA-METAL SERIES MODELS, TIMING AND MAGMA TYPES IN AND NEAR THE NEVADA TEST SITE.

Magma-Metal Series Class	Class Name	Age (Ma)	Metals
PC	Peraluminous Calcic	90–72?	Au-qtz veins; tungsten
MCAo	Metaluminous Calc-Alkalic, oxidized	96–93	Porphyry Cu-Mo
MCAr	Metaluminous Calc-Alkalic, reduced	15–13	Au, As, Sb, Hg, Tl
MACo	Metaluminous Alkali-Calcic oxidized	102–99	Ag, Pb, Zn
MACr	Metaluminous Alkali-Calcic reduced	14–11	Ag, Sn, F, Bi, LREE
MQA	Metaluminous Quartz Alkalic	10	Au, some Ag
MNA	Metaluminous, Nepheline Alkalic	< 8. 7	Te, Au?

the Gold Meadows stock, which is metaluminous calc-alkalic (MCA) at 93–96 Ma. The peraluminous systems can also be subdivided into two systems: peraluminous calcic (PC) tungsten associated with pegmatite dikes Late Cretaceous age and peraluminous calc-alkalic (PCA) gold-quartz veins at 85–72 Ma.

Metaluminous Climax (MAC) and Gold Meadows (MCA) Stocks

The Climax intrusive complex in the broader Oak Springs area (super system) and the Twin Ridge pluton south and east of the Climax mine near the Michigan Boy mine area described by Maldonado (1977, 1981) are MAC systems. Mineralization in these two systems consists of lead-zinc veins and associated tungsten deposits (MAC29B model). The Climax stock is dated by K-Ar biotite ages ranging from 91 to 101 Ma (Marvin and others, 1970; recalculated by Naeser and Maldonado, 1981) and with fission track ages on sphene and zircon ranging from 100 to 104 Ma (Naeser and Maldonado, 1981). The Climax stock cross cuts the upright to east-vergent, normally faulted folds and SSE-vergent fold thrusts (Houser and Poole, 1960). As the Belted Range thrust in the Belted Range projects directly toward the Climax stock, it is possible that the east- to SSE-vergent deformation intruded by the Climax stock is related to the Belted Range fold-thrust complex. This deformation is probably related to an early episode of the Sevier orogenic belt.

The combined MAC mineralization, petrochemistry, and association with east-to southeast-directed fold thrusting constitute a stratotectonic assemblage in the sense of Keith and Wilt (1986). This stratotectonic assemblage migrated eastward as part of the Sevier fold-thrust belt between 89–72 Ma (Armstrong, 1972). This stratotectonic pattern is earlier, but is similar to that documented by Keith and Wilt (1986) as the eastward-migrating Tombstone assemblage, affecting southeast Arizona and southwest New Mexico between 80 and 56 Ma.

The Gold Meadows stock is a slightly younger, metaluminous calc-alkalic (MCA) system. The Gold Meadows stock crops out west of the White Rock Springs copper-silver mineral system and is likely to be a MCA14C(?) model. The stock yielded 96–93 Ma dates (Naeser and Maldonado, 1981) and is a biotite granodiorite containing magnetite. In other areas, MCA biotite granodiorites are commonly associated with commercial copper-molybdenum-silver porphyry systems.

The northern Calico Hills mineralized area is several miles south of the White Rock Springs district and is dominated by copper-silver hosted in Paleozoic rocks. The area is also associated with anomalous arsenic, antimony, lead, mercury, and barium (as barite). This system is moderately anomalous in gold, zinc, and molybdenum (Castor and others, 1999; Quade and others, 1984; Simonds, 1989). No intrusive is exposed, but the copper-dominated, polymetallic aspect of the data is similar to some high-level, porphyry copper-polymetallic deposits of the MCA14L model.

The Calico Hills brucite area has some characteristics that are common to the more economic brucite skarns at Gabbs, Nevada. There, they are associated with strongly oxidized, biotite

Table 2. PRE-TERTIARY MAGMA-METAL SERIES MODELS, TIMING, AND MAGMA TYPES IN THE BROADER NEVADA TEST SITE REGION.

Magma-Metal Class	Age (Ma)	Metals	Character	Examples
PC2	90–72 ?	Au-qtz veins	Cpy, gal, hem	Trappmans district, Manhattan, Silver Peak district, Mineral Ridge (Mary mine), Chloride Cliff and Lee districts
PCA3A	98±27	W	W skarn, greisens, and veins	Tungsten Canyon, Fluorspar Canyon in southern Bare Mountain, Funeral Range
MCA16B?		Brucite $Mg(OH)_2$	Brucite skarn	Calico Hills brucite
MCA14L?		Cu-polymetallic-Ag	Stage 4, porphyry Cu?	Northern Calico Hills
MCA14C?		Cu, Mo, Ag	Porphyry Cu-Mo?	Gold Meadows stock near White Rock Springs Cu-Ag mineral system
MAC29B	102–99	Ag, Pb, Zn, Cu, Mo, W	Pb-Ag polymetallic veins in faults in Paleozoic sedimentary rocks	Climax stock, Twin Ridge plutons, Oak Springs super-system

granite plutons (MCA16B model). Both the northern Calico Hills and Calico Hills brucite occurrences are probably older than the alunitic, low level mercury mineralization hosted in the Miocene ash flow sequence to the immediate south and west of these Paleozoic-hosted, polymetallic-base-metal-brucite occurrences.

Peraluminous Magmatism and Features Associated with Flat Subduction

Peraluminous magmatism and related mineralization affected the area in the Late Cretaceous, although precise ages and geochemistry are lacking. However, mineral assemblages, metal contents, locally associated intrusive phases, and mid- to late Cretaceous metamorphic cooling ages suggest these models. The peraluminous magmatism can be subdivided into two components.

The older peraluminous event at Bare Mountain may be associated with tungsten mineralization in the Tungsten Canyon area of southern Bare Mountain (PCA3A model). In Tungsten Canyon, small pegmatitic intrusions (Monsen and others, 1990; Eng and others, 1996) may be associated with the tungsten mineralization. This system may correlate with better-constrained peraluminous granitoid intrusions in the Fluorspar Canyon area of northern Bare Mountain, where a muscovite granite yielded a U-Pb age of 98±27 Ma on zircon (Monsen and others, 1990, 1992). The pegmatites cross cut or radiometrically postdate the metaluminous event. The error on the muscovite granite age in northern Bare Mountain is large enough that the peraluminous sill postdates the metaluminous Gold-Acre stock, dated at about 93 Ma. The error bar allows the peraluminous magmatism at northern Bare Mountain to be as young as 71 Ma.

This peraluminous intrusion in northern Bare Mountain appears to be post-kinematic with respect to mid- to Late Cretaceous, WNW-directed (based on fabric data presented in Hoisch and Simpson, 1993) thrust faults that affected Paleozoic rocks at Bare Mountain. This peraluminous intrusion shares similarities with other post-kinematic two-mica granites elsewhere in the Great Basin (such as in the Snake Range). There, the granites are late kinematic and are locally associated with west-directed thrusting. Similar patterns occur in the Mojave-Sonora region as the Wilderness assemblage (Keith and Wilt, 1986) and in the Big Maria Mountains near Blythe in southeastern California (Hoisch and Simpson, 1993).

The west-directed tectonic fabric on northern Bare Mountain is kinematically consistent with thrust faults, such as the Panama thrust, that are correlated with the regional CP thrust system documented by Caskey and Schweickert (1992). This thrust system crosscuts earlier elements of the Sevier orogeny, specifically the Belted Range thrust system. Relative age relationships are consistent with the CP thrust being a late Laramide structural element related to west-directed, flat subduction.

Hydration of the lower crust (Jones and others, 2015) produced regional uplift by underplating serpentinized peridotite (Keith and others, 2008; Keith and Swan, 2010) and by dewatering oceanic asthenosphere. This regional uplift resulted in the Eocene erosion surface and uplift-cooling ages (typically Paleocene to Eocene) superimposed on older rocks.

In southwestern Nevada, these reduced ages may reflect regional uplift associated with flat subduction. At Bare Mountain, Monsen and others (1992) report 51.6±1.3 Ma on muscovite from schist in the Wood Canyon Formation. They obtained similar ages on basement schist (Wood Canyon Formation) that ranged between 44.3 and 48.6 Ma on muscovite-biotite pairs (Monsen and others, 1992). Cooling ages include fission-track apatite ages of 55.6±5.6 Ma on the Gold Meadows stock and 78.6±6.7 Ma on the Climax stock (Naeser and Maldonado, 1981). These ages are interpreted as the time when apatite cooled to below the annealing temperature of about 90°C.

Another suite of peraluminous magmatism may be associated with gold-quartz veins hosted in Late Proterozoic/Paleozoic sedimentary rocks at Chloride Cliff, Lee, Echo Canyon-Lee's Camp, and the Johnnie districts. These are provisionally considered to represent PC2 models, as direct evidence for igneous intrusions is lacking. Mineral assemblages consist of local chalcopyrite, galena, and specularite associated with gold-quartz. This mineral assemblage is similar to those associated with PC2 models in the Panamint Range to the west (such as Skidoo, Ballarat, Suitcase, and Briggs). Trappmans district, which is about 50 miles north of Yucca Mountain, is more clearly associated with peraluminous granitic rocks. By analogy with the better-dated Panamint occurrences (especially Ballarat and Skidoo that are associated with the Hall Canyon and Skidoo plutons, respectively), the Chloride Cliff and Lee districts could belong to a 85–72 Ma interval.

An apparent magma gap occurs between approximately 72 Ma and 17 Ma in the region surrounding the Nevada Test Site. No igneous, metallogenic, or deformational events are recorded in the Yucca Mountain region until mid-Miocene time.

Early Tertiary(?) Carbonaceous Shales Associated with Flat Subduction

During the previous 15 years, Keith and associates have developed an ultra-deep hydrocarbon (UDH) or hydrothermal oil concept with case studies throughout the world. UDH processes may have occurred in southwestern Nevada during flat subduction at the end of the Laramide. Underplating of serpentinized peridotite and associated hydrothermal activity may have led to the formation of high-density chemical brines that ultimately erupted at the surface as chemical-mud volcanism. The UDH model for a flat subduction setting is shown on Figure 3. The UDH process involves deep-sourced, hydrocarbon- and magnesium-rich brines that were formed by serpentinization of flatly subducted, harzburgitic peridotite. The brines were subsequently emplaced into lacustrine, exhalative, lake environments during the Eocene (55–43 Ma), similar to the Green River Formation (Johnston and others, 2010).

The UDH model is based on the concept that serpentinization and hydrocarbon occurrence are related (Fruh-Green and others, 2004; Hazen and others, 2012). Recent analyses have identified kerogen in meteoritic materials, mantle olivine materials, serpentine, talc, hydrothermal dolomite, Herkimer quartz, fluid inclusions in igneous rocks, diamonds, and graphite schist, in addition to the conventional black shales and petroleum source rocks in supercrustal sedimentary basins. Hydrocarbons are commonly associated with hydrothermal Mississippi-Valley-type deposits and with Carlin-type deposits. Herkimer quartz contains textures that show, within single quartz crystals, a complete sequence of oil generation from platy kerogen starter through globulated, volatilizing kerogen, to liquid oil. The hydrothermal setting for oil has been experimentally validated by Lewan (1997), who could only make oil in the presence of hydrothermal water interacting with kerogen-rich shales between 310° and 380°C.

In the UDH model, massive magnesium- and kerogen-charged brines are produced by serpentinization of peridotite and are transported into the upper crust as low-density, supercritical fluids. When these fluids reach the upper crust and ionize, rapid reactions occur to hydrogenate kerogen and produce hydrothermal oil. The hydrogen is released from water when mineral reactions create oxygen-rich minerals, such as dolomite, quartz, and clay. Oil is directly made in the reservoir environment and is not transported to it from burial of kerogen-rich source rocks.

The hydrothermal oil model explains two problems for the conventional model of oil formation: 1) where does the hydrogen come from that would hydrogenate the hydrogen-poor ker-

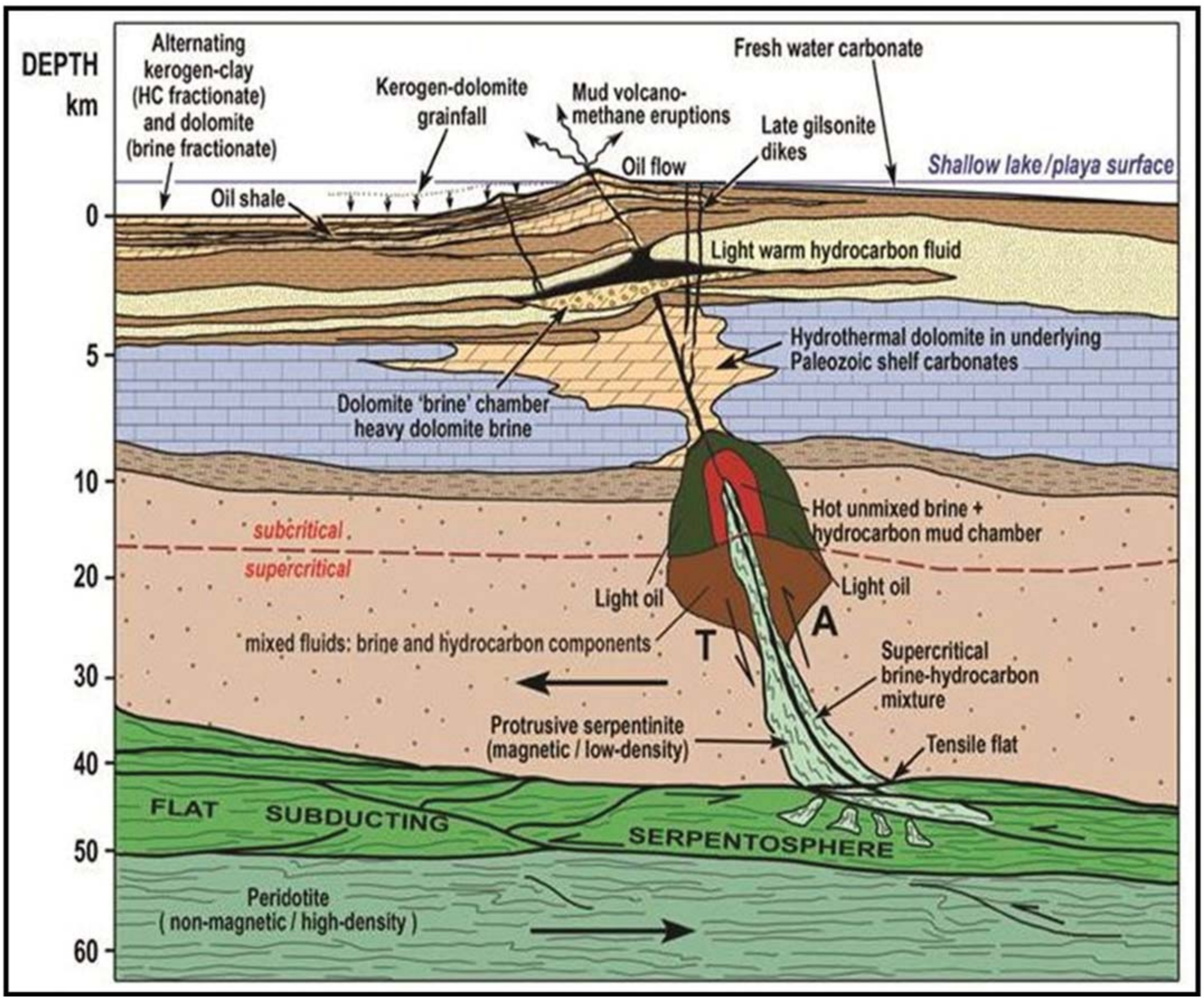

Figure 3. Schematic diagram of the UDH model in flat subduction settings showing development of deep-sourced, hydrocarbon- and magnesium-rich brines formed by serpentinization of flatly subducting, harzburgitic peridotite.

ogen; and 2) where is the hydrocarbon trail from the presumed hydrocarbon source rock to the trap site. The source of hydrogen is solved by the hydrothermal process, in which abundant amounts of hydrogen are supplied by water breakdown to make coeval, oxygen-rich minerals. The second problem is solved by the hydrothermal plume, which leaves an alteration trail from the hydrothermal brine.

These brines do not stop after the hydrothermal oil is formed in the reservoir. They keep going to breach the crust/atmosphere or hydrosphere interface. The brines erupt as extensive, chemical mud "volcanism". Examples are the modern mud volcanos in the Caspian Sea region. The products of mud "volcanism" are deposited as carbonaceous black shale. Oil shales are present in the Elko Formation and the Sheep Canyon Formation to the north of the NTS (French, 1997). French correlated these formations with rocks of Joshua Hollow, (labeled Horse Spring Fm. in Figure 2) which were deposited between the Paleozoic section and the volcanics of the Southwest Nevada Volcanic Field at Bare Mountain.

Rocks equivalent to those of Joshua Hollow occur in the same general area as the west-vergent CP Thrust system (as shown in Caskey and Schweickert, 1992). There might be a genetic association between the west-directed CP thrust system and the rocks of Joshua Hollow and their equivalents. The carbonaceous material in the rocks of Joshua Hollow yielded TOC values up to 1.59 wt% (French, 1997).

The oil shales of the Green River Formation may be a possible example of the flat subduction UDH model. These oil shales are associated with deep-seated, southwest-vergent, thrust uplifts, such as the Wind River Uplift in Wyoming and the Uintah Uplift in Utah. The Wind River thrust fault has been shown seismically to penetrate to the base of the crust, where it would have had access to the serpentosphere (layer of serpentinized peridotite). These deeply penetrating, southwest-vergent faults could have tapped into a UDH process. The high-density brines that were charged with kerogen and magnesium rose as a plume from deeper serpentinite diapirs to produce extensive chemical muds, including oil shales. These seeps were a source of food for numerous animals, much like the modern white smokers that are surrounded by tube worms. When the seep emitted excess methane or acids, it produced a 'kill zone' that left layers of abundant fish fossils in certain layers of the lake beds.

TERTIARY MAGMATISM, TECTONISM, AND MINERALIZATION

Southern Great Basin Tectonism

At 43 Ma, change in the magmatic-tectonic framework in southwestern North America may have been triggered by the collision of India with southern Asia. This collision produced a dramatic slowing and change in direction of subducting plates beneath southwestern North America. The subducting slab began to gravitationally collapse and the direction of subduction shifted from E-W to NE. The steepening subducting slab involved a rapid trenchward migration of the arc. In the Great Basin, a WNW-trending arc segment migrated to the SSW from Eocene to about 7 Ma (Stewart and Carlson, 1976; Stewart, 1980).

The MCA facies of the arc system and its associated copper-gold mineralization were overprinted approximately 5 to 10 million years later by the southward migrating, MAC units of the middle part of the arc system and its associated lead-zinc-silver ± tin deposits. The MAC units comprise the main volume of volcanic rocks and represent the thermal axis of the magmatic arc. The passage of the arc thermal axis is a tectonic trigger for kinematic activity on earlier tectonic elements as the arc transgresses through an area.

The stress-strain regime that accompanied the Miocene arc passage was regional NNE-SSW compression. This compression and the influence of the thermal axis acted on pre-existing northwest-striking structural elements, such as the Walker Lane and Las Vegas shear zones, to produce recurring right-slip motion. The compression acted on pre-existing northeast-striking structural elements, such as the Spotted Range-Mine Mountain zone of Carr (1990) to produce left-slip motion. This compression acted on NNE-striking faults with tension to produce dip-slip motion. This pattern of intra-arc transtension migrated southward with the arc and was most active in the area of the MAC arc thermal axis.

Tectonic Framework of the Southwest Nevada Volcanic Field

A discussion of the Miocene tectonic framework for the Southwest Nevada Volcanic Field (Figure 4) is useful to understand the emplacement of the volcanic rocks and mineralization. The Paintbrush/Timber Mountain sequence was emplaced into regional, strike-slip tectonics. Within this framework, north-south to NNE-striking, tensional zones provided dilational jogs between the strike-slip fault elements. A major NNE-trending dilational jog is inferred to exist between the south-southeastern end of the Walker Lane fault zone north of Pahute Mesa and the Pahrump-Stateline/Las Vegas Valley shear system to the southeast. In effect, the NNE-striking zone shown on Figure 4 serves as a strain transfer mechanism to accommodate differential stress between the Walker Lane zone on the north and the Las Vegas/Pahrump-Stateline fault system to the south. The line of gravity lows defining the Kawich-Greenwater rift (as delineated by Carr, 1990) is one of the main elements of the tensional jog.

The Kawich-Greenwater rift is a Miocene-age, arc-related, strike-slip, pull-apart basin that was pervasively intruded by a large trachybasalt magma body. In the surface geology, the Kawich-Greenwater gravity low is shown by a NNE-trending swarm of normal faults that are north and south of the Timber Mountain-Oasis Valley Caldera Complex (Carr, 1990). The fault swarm coincides with the NNE-trending axis of calderas and relates to the sources of the Paintbrush and Timber Moun-

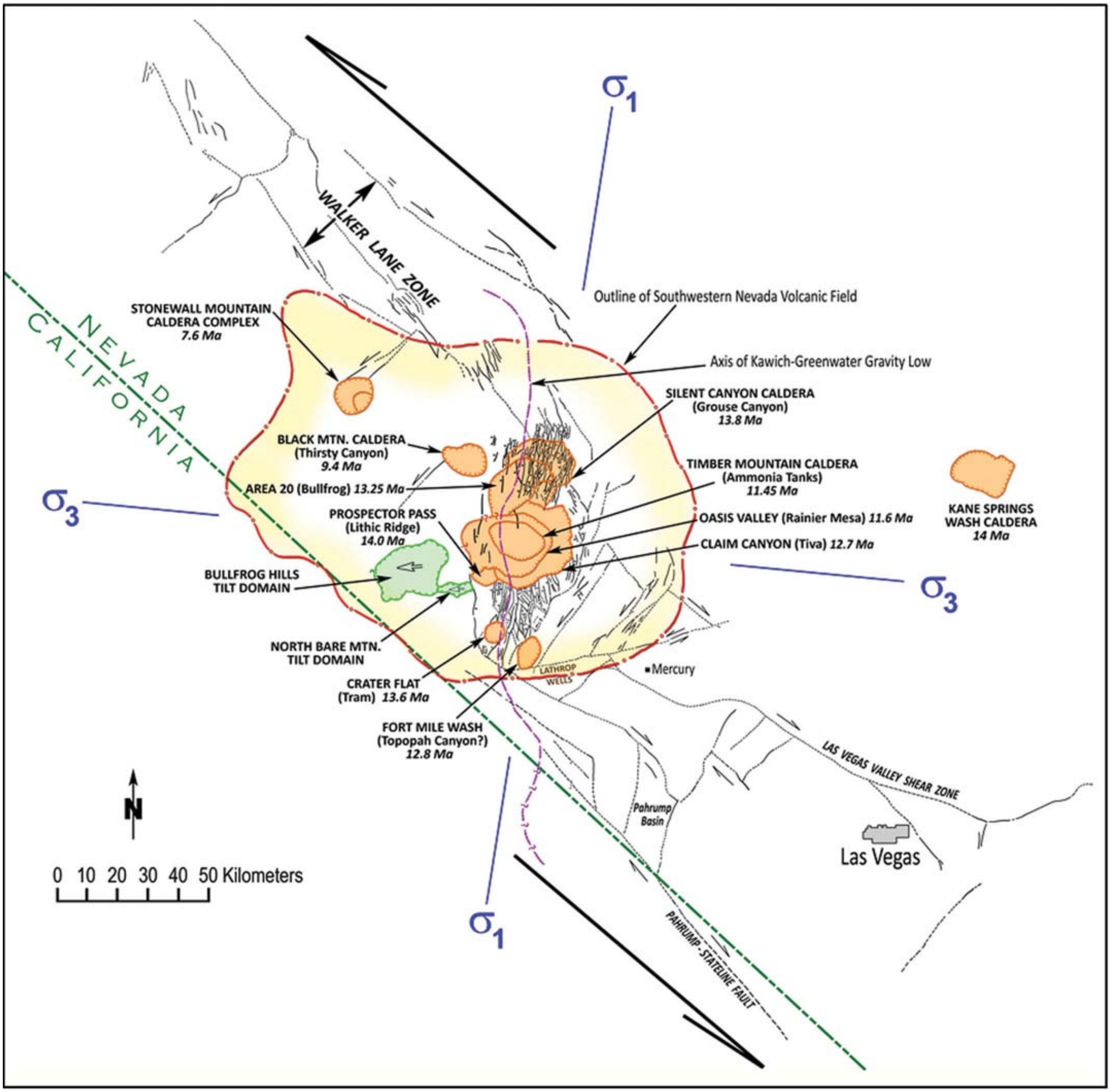

Figure 4. Map of structural elements and volcanic centers in southwestern Nevada.

tain volcanics. The western margin of the rift is a composite of the Bare Mountain down-to-the-east fault and other normal faults that coincide with the western margin of the Silent Canyon caldera to the north. The eastern margin is a composite of faults underlying Forty Mile Wash, the Paintbrush fault, and down-to-the-west faults on the eastern margin of the Silent Canyon caldera. In between these boundary faults is an anastomosing swarm of normal-slip, high-angle, NNE-striking normal faults.

During a magmatic lull between the eruption of the Paintbrush Group and the Timber Mountain Group, low-angle, normal, "detachment" faulting occurred in the Bullfrog Hills and northern Bare Mountain between 12.7 and 11.6 Ma (Sawyer and others, 1994). We interpret the "detachment" faulting as denudation faults that are a local, gravitationally induced, mega-landslide feature developed on previous thrust faults on a broad, westward inclined ramp (shown in Carr, 1990). This ramp flanked a north-south domal axis within the Kawich-Greenwater rift. The north-trending domal feature may have been formed as the underlying batholith rose into its culmination beneath Timber Mountain just prior to the eruptions of the Rainier Mesa and Timber Mountain Tuffs. In this view, the Bare Mountain/Bullfrog denudation fault is not a manifestation of regional extension, but rather is a subordinate and local, distensional feature related to arc-related transtension. The passage of the central part of the arc (the thermal axis) through southwestern Nevada triggered this transtension between 14 and 11.4 Ma.

The transtensional, intra-arc tectonic framework for the Yucca Mountain region was an important control on the "plumbing-system" for hydrothermal fluids. The dilational jog that coincides with the NNE-striking, high-angle fault swarms is a deep-seated feature. The fault swarms, thus, are deeply penetrating features that do not flatten downward into a regional, extensionally produced, denudation fault. Within the Nevada Test Site region, seismic data provide strong evidence that the high-angle faults penetrate at least to 7,000 feet (Brocher and others, 1996, 1998; Brocher and Hunter, 1996). These high-angle faults appear to offset the Paleozoic-Cenozoic contact between about 3,000 and 7,000 feet.

Within the fault swarm, there are alternating domains of low-density and high-density fracturing (Scott, 1990). The deep-seated faults provided conduits for fluids derived from deep-seated plutonic sources of the Paintbrush and Timber Mountain volcanic rocks.

MIOCENE MAGMATISM AND MINERALIZATION

Three-fourths of the mineral systems present in the region in and around the Nevada Test Site are related to the Miocene arc system (Table 3 and Figure 1). Mineralization records increasingly alkaline magma-metal series models with decreasing age, which is a result of steepening subducting slab during the Miocene. The principal magmatic features of the Miocene arc in the Nevada Test Site region are the large-volume ash sheets that were erupted from the Timber Mountain Caldera complex between 14 and 11.45 Ma (Sawyer and others, 1994). The Paintbrush/Timber Mountain sequence is MAC (Figure 1), which throughout the world is associated with lead-zinc-silver±tin mineralization (Keith and others, 1991; Wilt, 1993). Copper and gold have only been produced as a byproduct from these systems.

Early Miocene, Au-As-Sb-Hg-Tl Mineralization (MCA12)

The earliest Miocene mineralization in the region is probably associated with calc-alkalic facies of the magmatic arc. Possible calc-alkalic igneous rocks are represented by hornblende-biotite diorite dikes on the east side of Bare Mountain, and by a 15 km long swarm of dikes mapped as quartz-latite porphyry dikes by Monsen and others (1990). In particular, the quartz-latite porphyry dikes display a spatial association with gold deposits at the Mother Lode, Sterling, and Diamond Queen mines. This gold mineralization carries the mercury, antimony, arsenic, and thallium signature that is considered by many to be a trademark of the sediment-hosted Carlin-type model (MCA12 model) or the closely related volcanic-hosted Round Mountain type model (MCA9 model). Textures of arsenic-rich rims around pyrite grains shown with back-scattered SEM imagery at the Sterling mine (Castor and others, 1999) also support the MCA model. In addition to the MCA12 gold models exposed on the east side of Bare Mountain, borehole UE-25 p#1 at Yucca Mountain intercepted low-level gold mineralization with Carlin-type trace-element signatures in the Lone Mountain Dolomite below about 4800 feet (Castor and others, 1999).

Ages on the early MCA ENE-striking hornblende diorite dikes at Bare Mountain include 26±1.7 Ma on hornblende and 16.6 Ma on biotite (Monsen and others, 1992). Altered possible equivalents of these dikes have yielded two K-Ar age dates of 14.9±0.5 Ma and 13.8±0.2 Ma (Marvin and others, 1989; Noble and others, 1991; Monsen and others, 1992). These dikes locally host gold mineralization at the MCA12 Mother Lode mine. The Mother Lode mine is hosted in the Joshua Hollow sedimentary sequence, which occurs at the base of the mid-Tertiary section at Bare Mountain (Eng and others, 1996). No mineralization with the geochemical signature characteristic of the MCA12 or MCA9 models (arsenic, antimony, mercury, thallium, gold metal signature) has been reported from volcanics younger than 14 Ma throughout the Yucca Mountain region, despite intense sampling. We infer that the MCA12 Carlin-type deposits were formed in the Yucca Mountain region between about 17 and 14 Ma.

The interpretation for an early age for the Carlin-type mineralization differs from interpretations that it was emplaced around 12.9 Ma as proposed by Castor and others (1999) and Weiss and others (1995). Our interpretation is based on relations at the Diamond Queen mine, which contains two mineralization events: a breccia mineralization that overprints an earlier dike-related mineralization, as shown in the geochemical data of mineralized samples. At the Diamond Queen mine, fluorite-bearing breccia contains clasts of altered quartz latite porphyry. Data from those clasts (Castor and others, 1999) contain elevated gold and other element signatures typical of Carlin-type deposits, but do not contain anomalous lithium, fluorine, or gallium, that are trademark signatures of the younger MAC mineralization models throughout the Nevada Test Site region. These data suggest that a pre-existing gold event associated with the quartz latite dikes was subsequently dismembered and mineralized by an overprinting event with a F-Li-Hg signature related to the regionally widespread MAC18D models that appear about 2 Ma later in this area. Mineralogically abundant fluorite and highly anomalous fluorine geochemistry are not known to occur in any other Carlin-type mineralization within the magma-metal series global data base. Thus, it is likely that the Sterling/Mary/Diamond Queen mine areas experienced two events closely spaced in time, but distinctly different in magmatic and metallogenic origin.

Table 3. TERTIARY MODELS, TIMING, AND MAGMA TYPES IN THE BROADER NEVADA TEST SITE REGION.

Magma-Metal Class	Age (Ma)	Metals	Magmatic Sequence: Cycle	Examples
UDH?	Post-5	Hydrothermal oil? and dolomite	Basin and Range basalts; no biotite; anhydrous	Thirsty Mesa, basalt of Amargosa Valley, basaltic andesite of Buckboard Mesa, Quaternary basalt of Crater Flat, basalt of Sleeping Butte, and Lathrop Wells volcanic center
MNA46	Younger than 8.7 Ma	Au-Te-Th-F-LREE; Mo-U	Terminal arc magmatism: leucite basanite; quartz deficient nepheline alkaline	Northern Bare Mountain (Daisy mine), Oasis Mountain area, central Clarkdale area; north of Rainbow Mountain, north of Montgomery Mountain; Life Preserver mine in Tolicha district
MQA35	10	Epithermal Au-Ag-Be-F; Au in quartz veins in NNW faults, electrum, adularia, sericite; low As, Sb, Hg, Tl	Rainbow Mountain sequence	Bullfrog district (Bullfrog, Montgomery-Shoshone, Original Bullfrog, Gold Bar, Mayflower-Pioneer mines); Bonanza Mountain area, Clarkdale and Tolicha districts
MAC18B	11.4	Sn/ polymetallic; sparse fluorite; qtz-calcite vnlts with As, Bi, Ga, Mo, Te, Tl	Fleur de Lis cycle in Paintbrush/ Timber Mountain sequence	Mafic magmas; Dome Mountain; Fleur de Lis Ranch area; Sleeping Butte; Transvaal Hills,
MAC18D	11.45	Hg-Li-F; alunitic alteration	Ammonia Tanks cycle in Paintbrush/ Timber Mountain sequence	Buttonhook Wash, Mine Mountain southwest, Calico Hills; Fatigue Wash area?; Solitario Canyon area; associated with magnetic highs
MAC18D	11.6	Moderately productive Au-Ag in Bullfrog Hills; Hg-Li-F; Ba, alunite, Th?	Rainier Mesa cycle in Paintbrush/ Timber Mountain sequence	Bullfrog Hills landslide mass; altered areas above, S, or E of magnetic high anomalies
MAC	12.8–12.7	No metals	Tiva cycle in Paintbrush/Timber Mountain sequence	From Claim Canyon caldron
MAC18B	12.8	Hot spring Sn; distal zone Zn-Tl-Bi-Pb-F-Ga-As-polymetallic	Topopah Spring cycle in Paintbrush/ Timber Mountain sequence	Quartz latite member of Topopah Spring Tuff is associated with fault-related, hot-spring vents (Abandoned Wash)
MAC17?	12.9–12.7	Elevated trace Ag, As, Au, Bi; moderately elevated Li, weakly elevated W, Zn, Sb, Pb, Hg, Se, Sn?	post-Wahmonie cycle in Paintbrush/ Timber Mountain sequence	Altered area in Wahmonie Formation; suggestive of epithermal Ag veins; adularia dated at 12.6±0.4 and 12.9±0.4
MAC18B	< 13.25	Zeolite-clay alteration; veins of specular hematite or MnOxide locally; pyrite, barite locally present	post-Prow Pass cycle in Paintbrush/ Timber Mountain sequence	Vein-type mineralization cutting units below the Calico Hills unit in boreholes in Yucca Mountain
MAC	13.25	—	Bullfrog Tuff cycle in Paintbrush/ Timber Mountain cycle	
MAC18B	14–13.25	Hot spring Sn mineralization: Weak As, Bi, Zn, W, Li, Pb, Sb, Tl, LREE	Tram cycle in Paintbrush/Timber Mountain sequence	Northern Yucca Mountain, Tram-Bullfrog contact
MAC18B?	14	Zeolite clay alteration, illite/smectite ± albite ± adularia ± chlorite ± sericite ± hematite±MnO	Lithic Ridge cycle in Paintbrush/ Timber Mountain sequence	Pyritic mineralization in the Tram Tuff
MAC	15.25–14.9	None; small volume ash flows		Redrock Valley Tuff, tuff of Yucca flat, Tub Spring Tuff, Tunnel Formation
MCA12	13.8–14.9 dikes; 17–14	Au, As, Sb, Hg, Tl, Se, Te; sedimentary rock hosted Au	Early Miocene	Eastern Bare Mountain, Sterling, Mother Lode, Diamond Queen mines, Joshua Hollow prospect; Yucca Mountain well UE-25 p#1 at 4858 ft. in Silurian Lone Mountain Fm.

Thermal Axis of the Metaluminous Alkali Calcic (MAC) Arc

The central part or thermal axis of the magmatic arc arrived in the Nevada Test Site area as extensive MAC volcanism after about 15–14 Ma. The first MAC volcanics are the Redrock Valley Tuff, the tuff of Yucca Flat, the Tub Spring Tuff, and the Tunnel Formation (Sawyer and others, 1994). These small-volume ash flow tuff units were erupted between 15.25 and 14.9 Ma from uncertain sources. No mineralization is known to be associated with these units.

Mineral systems in the Yucca Mountain and Nevada Test Site region can be correlated with cycles in the Paintbrush and Timber Mountain groups. The pertinent volcanic units include the following:

- Lithic Ridge Tuff (14 Ma) [MAC18B];
- Crater Flat Group, which includes the Tram Tuff (14–13.25 Ma) [MAC18B], Bullfrog Tuff (13.25 Ma), and the Prow Pass Tuff;
- Post-Prow Pass interval (< 13.25 Ma) [MAC18B];
- Wahmonie Formation (13 Ma);
- Post-Wahmonie interval (12.9–12.7 Ma) [MAC17];
- Calico Hills Formation (12.9 Ma);
- Paintbrush Group, which includes the Topopah Spring cycle (12.8 Ma) [MAC18B], Pah Canyon Tuff, Yucca Mountain Tuff, and Tiva Canyon Tuff cycle (12.8–12.7 Ma);
- Timber Mountain Group, which includes the Rainier Mesa Tuff (11.6 Ma) [MAC18D] and Ammonia Tanks Tuff (11.45 Ma) [MAC18D]; and
- Fleur de Lis cycle (11.4 Ma).

Lithic Ridge Cycle (14 Ma), Pyrite in Clasts in Tram Tuff (MAC18B)

The Lithic Ridge Tuff may have erupted at 14 Ma from a small caldera source in the vicinity of Prospector Pass. Pyritic mineralization is contained in clasts in the Tram Tuff (Castor and others, 1999; Weiss and others, 1996, 1995) and may represent a now-dismembered mineralized system containing pyrite. Trace elements in the pyritic tuff are the same metal assemblage as the surface samples associated with tin mineralization at the top of the Topopah Springs Tuff. Pyritic clasts in the Tram Tuff may be from the same tin-related model (MAC18B) as the other mineral occurrences.

Tram Cycle (14–13.25 Ma), Hot Spring Sn Mineralization (MAC18B)

Castor and others (1999) sampled a paleo-hot spring or fumarolic horizon along the Tram Tuff-Bullfrog Tuff contact in northern Yucca Mountain. They interpreted the silicified ledges as hydrothermal silica deposited by hot springs on a paleosurface at the top of the Tram Tuff. Samples collected from these ledges contain weakly elevated levels of arsenic, bismuth, zinc, tungsten, lithium, lead, antimony, and slightly elevated levels of thallium and light rare earth elements (Castor and others, 1999). The silicified ledges are assigned to the MAC18B model.

Bullfrog Cycle (13.25 Ma)

Shortly after the close of the Tram cycle at about 13.5 Ma, a widespread, moderate-volume (650 km^3), ash-flow sequence, named the Bullfrog Tuff, was erupted from the vicinity of the Area 20 caldera (Sawyer and others, 1994). Following the eruption of the Bullfrog Tuff Member, the Prow Pass Tuff was erupted between 13.25 Ma and 13.0 Ma.

Post-Prow Pass (< 13.25 Ma), Vein Mineralization (MAC18B)

After eruption of the Prow Pass Tuff, a widespread mineralization event affected the Prow Pass Tuff and earlier units at Yucca Mountain. A vein-type mineralization cuts units below the Calico Hills unit within boreholes at Yucca Mountain. This mineralization contains zeolite-clay alteration of analcime, which occurs in quartz±calcite± fluorite veins. Additional minerals include illite/smectite, albite, adularia, chlorite, sericite, specular hematite, pyrite, and barite, with slightly elevated antimony, arsenic and molybdenum, with some thallium, mercury, selenium, lead, and zinc (Castor and others, 1999).These characteristics are similar to alteration and mineralization locally associated with anomalous tin occurrences in hot springs at the top of the Topopah Springs Tuff of the Paintbrush Group. The MAC18B mineralization may represent veins from the same hydrothermal plume as that vented in the hot springs.

Post-Wahmonie 12.9–12.7 Ma, Epithermal Ag Mineralization (MAC17)

After eruption of the Prow Pass Tuff of the Crater Flat Group, andesitic volcanism erupted in the vicinity of the Wahmonie Hills to produce lavas, tuffs, and breccias of the Wahmonie Formation (Sawyer and others, 1994). The area was subsequently intruded by a series of porphyritic granodioritic intrusions (Castor and others, 1999).

Alteration is dominated by adularia-sericite-silica. The silver content and adularia-sericite alteration are characteristic of the epithermal silver vein model (MAC17). The silver mineralization in the Wahmonie Hills has been directly dated, with adularia yielding two K-Ar dates of 12.6 Ma±0.4 and 12.9±0.4 Ma (Jackson, 1988; Weiss and others, 1995).The Wahmonie system may be associated with magmatism that was much wetter than the magmatism intruded within the Timber Mountain caldera complex emplaced along the Kawich-Greenwater axis. The assimilation of a more fluid-rich source is supported by isotopic data reported in Farmer and others (1991).

Topopah Spring cycle (12.8 Ma), Hot Spring Sn Mineralization (MAC18B)

After formation of the Wahmonie volcanic center, tuffs and lavas of Calico Hills were erupted around 12.9 Ma and the Topopah Spring Tuff was erupted at 12.8 Ma. The quartz latite member of the Topopah Spring Tuff is associated with a cluster of fault-related, hot spring vents that are well developed within Yucca Mountain. This mineral system contained an ore-grade tin occurrence in a float sample near Abandoned Wash, about one mile south of borehole USW G-3 (Castor and others, 1999).

In the Topopah Spring Tuff, a northern distal zone is slightly enriched in Zn-Tl-Bi-Pb-F-Ga-As, whereas a southern proximal zone has elevated Sn and W. The hot spring tin mineralization has been called a fumarolic horizon at the top of the Topopah Spring Tuff. The Pah Canyon Tuff unconformably buried the fumarolic horizon (Barr and others, 1996) between 12.8 Ma and 12.7 Ma, which are the dates on the underlying Topopah Spring and the overlying Tiva Canyon units by $^{40}Ar/^{39}Ar$ techniques (Sawyer and others, 1994).

Physical features exposed in the Exploratory Studies Facility [ESF], a pilot adit for the Yucca Mountain proposed radioactive waste repository), suggest that this mineralization is related to hot springs rather than fumaroles. Recurrent faulting postdated the hot spring event and the overlying biotite-bearing bedded tuff. Barr and others (1996), Levy and others (1996), and Peterman and others (1996) observed structural disruption following the hydrothermal effects. The underlying magmatic sequence at Yucca Mountain is more hydrous than magmatic sequences associated with fumarolic activity. The Topopah Springs Tuff contains a significant biotite component, in contrast to tuffs associated with fumarolic deposits, such as the Valley of Ten Thousand Smokes in Alaska (Papike and others, 1991). Anomalous values of tin, tungsten, iron, and bismuth occur along the Busted Butte fault system south of the Dune Wash fault, which partly corresponds with a strong magnetic low.

Tiva Cycle (12.8–12.7 Ma)

Volcanic activity shifted to the north and the Tiva Canyon Tuff was erupted from the Claim Canyon caldron at 12.8 Ma (Sawyer and others, 1994). The Tiva ash-flow tuff erupted from a previously zoned magma chamber (Lipman and others, 1966; Schuraytz and others, 1989; Flood and others, 1989), Broxton and others, 1989; Warren and others, 1989). Mineralization is not associated with the quartz latite member of the Tiva. The Tiva Canyon Tuff was the driest of the ash-flow sheets erupted during the Paintbrush/Timber Mountain magmatic sequence (data in Warren and others, 1989).

Rainier Mesa Cycle (11.6 Ma), Hg-F-Li Mineralization (MAC18D)

After a pause of 1.8 million years, the Rainier Mesa Tuff was erupted at about 11.6 Ma (Sawyer and others, 1994). Pre-Rainier Mesa tectonism was associated with rise of silicic magma beneath the Timber Mountain portion of the Kawich-Greenwater gravity low. This doming may have induced large-scale landslides in the northern Bare Mountain and Bullfrog Hills. This gravitational sliding produced the distinctive tilt patterns that have been extensively reported as listric faulting. Magmatism of the Rainbow Mountain Group is associated with moderately productive gold-silver deposits emplaced into the landslide mass in the Bullfrog Hills.

At 11.6 Ma (Sawyer and others, 1994), large amounts of Rainier Mesa Tuff were erupted from the Oasis Valley caldera (Carr, 1990). The Rainier Mesa Tuff contains much more magnetite than underlying units (Broxton and others, 1989). The magnetic anomalies are associated with known faults or with caldera ring margins (Feighner and others, 1996) and correlate with alunitic alteration associated with the MAC18D mercury-fluorine-lithium model. These altered areas consistently occur above, south and/or east of many magnetic highs.

The higher abundance of biotite in the Rainier Mesa Tuff correlates with a higher frequency of mineralization. The MAC18D model is the most frequent mineral system present in the Yucca Mountain area. Of the 40 mineral systems in the region (Figure 1), most fit the MAC18D model. The MAC18D model contains higher frequencies and higher average element contents of mercury, lithium, fluorine, and barium than the tin-related MAC18B model. Abundant alunite is present in the MAC18D model and is conspicuous by its absence in the tin-related MAC18B model. Adularia and carbonate are less common in the MAC18D model.

Ammonia Tanks Cycle (11.45 Ma), Hg-F-Li Mineralization (MAC18D)

The Ammonia Tanks Tuff was erupted from the Timber Mountain caldera as a rhyolite-quartz latite magma with MAC affinity (Figure 5). The MAC18D systems (Buttonhook Wash, Mine Mountain southwest, and the Calico Hills systems) either yield reliable K-Ar alunite dates younger than the Ammonia Tanks dates and/or crosscut the Ammonia Tanks stratigraphic unit. The Ammonia Tanks-related mineralization contains alunitic alteration, locally elevated mercury-lithium-fluorine, and a spatial association with well-defined magnetic highs.

Fleur de Lis Cycle (11.4 Ma), Sn/polymetallic Mineralization (MAC18B)

Volcanism waned after eruption of the Ammonia Tanks Tuff, although a series of basalts and basaltic andesites erupted at Dome Mountain. The sequence consists of a lower basalt with K-Ar whole-rock dates ranging from 10.7 to 10.1 Ma (Fleck and others, 1991). These mafic rocks indicate that the silicic magmas were evacuated from their batholith-scale magma chambers and/or the majority of the silicic component of the underlying batholith had largely crystallized (Broxton and others, 1989).

Slightly prior to the eruption of the Dome Mountain mafic magmas, small amounts of rhyolite tuffs erupted at around11.4 Ma (K-Ar dates in Sawyer and others, 1994) in the northwestern part of the Timber Mountain caldera complex near Fleur de Lis Ranch. Late stage rhyolitic tuffs were also erupted near Sleeping Butte. In the Thirsty Canyon area, felsic volcanic rocks and interbedded siltstone and sandstone are altered by fine-grained silica. Sparse drusy fluorite is locally present with quartz and calcite in veinlets that cut highly fractured and sheared rhyolite lavas. These veins contain elevated concentrations of arsenic, bismuth, gallium, molybdenum, tellurium, and thallium (Castor and others, 1999), which are characteristic of the tin-related MAC18B model.

Two systems are present in the Transvaal Hills. The Buttonhook Wash system consists of oxidized, acid-sulfate, alunite-bearing rocks associated with the later part of the Ammonia Tanks Tuff. About 1 km west of Buttonhook Wash, most of the historical workings are along steeply dipping, N to NE-striking normal faults associated with areas of argillic and zeolitic alteration. At the principal shaft south of the Transvaal site, weakly elevated gold, bismuth, molybdenum ± thallium ± tin geochemistry has been reported in Tingley and others (1996, 1998). Generally, only very weakly elevated concentrations of mercury have been obtained from the western part of the Transvaal district (Tingley and others, 1996, 1998). This low-sulfur, adularia-clay alteration is characteristic of the MAC18B tin-related model.

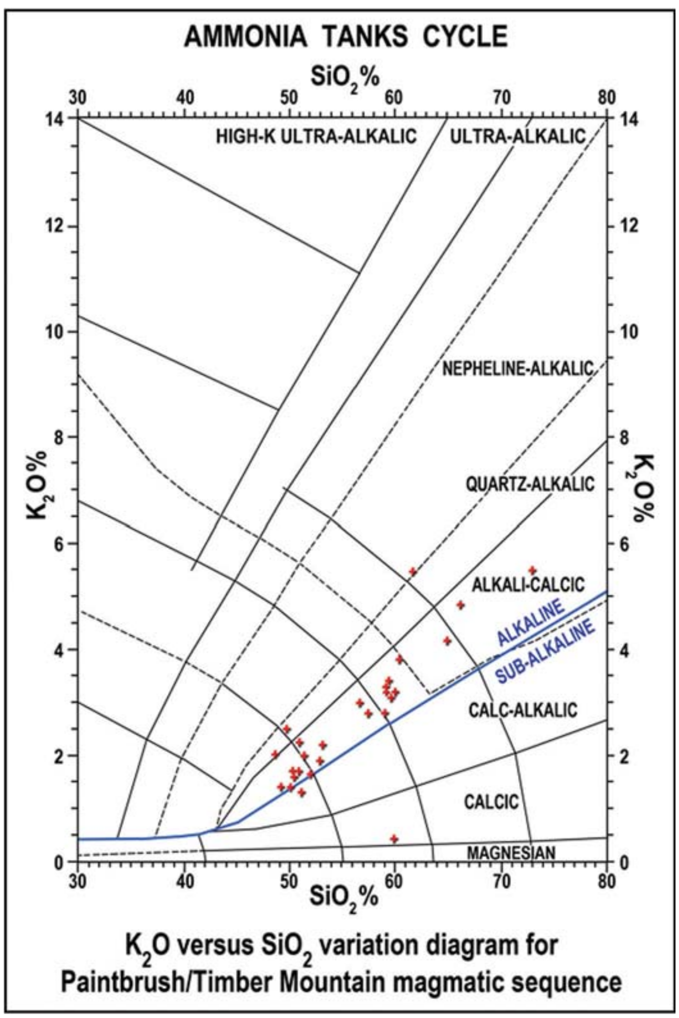

Figure 5. K_2O versus SiO_2 variation diagram for Paintbrush/Timber Mountain magmatic sequence.

Late Arc, Quartz Alkalic Magmatism (MQA)

A major shift in the petrochemical structure of the arc sequence took place in the vicinity of the Nevada Test site at about 10.5 Ma. Quartz alkalic (MQA) magma-metal series rocks erupted west of Timber Mountain caldera from the Bullfrog Hills to Stonewall Mountain. Within the Bullfrog Hills, basaltic lavas (basalt lava number 4 of Ransome, 1910; Eng and others, 1996) represent the first appearance of MQA rocks from the Black Mountain caldera and lavas sourced in the Stonewall Mountain caldera (Figure 6).

Post-10.5 Ma, Epithermal Au-Ag-Be-F Mineralization (MQA35)

Widespread mineralization in the Bullfrog Hills is temporally associated with the latitic and high-K, high-silica rhyolite and hypabyssal intrusives within the Rainbow Mountain sequence. Adularia-sericite stable, gold-silver epithermal deposits are spatially associated with the MQA magmatic centers. They are characterized by local fluorine-beryllium anomalies and generally low to erratic arsenic, antimony, mercury and thallium values. Examples include the Clarkdale district, eastern Tolicha district, Mayflower-Pioneer mines, North Bullfrog,

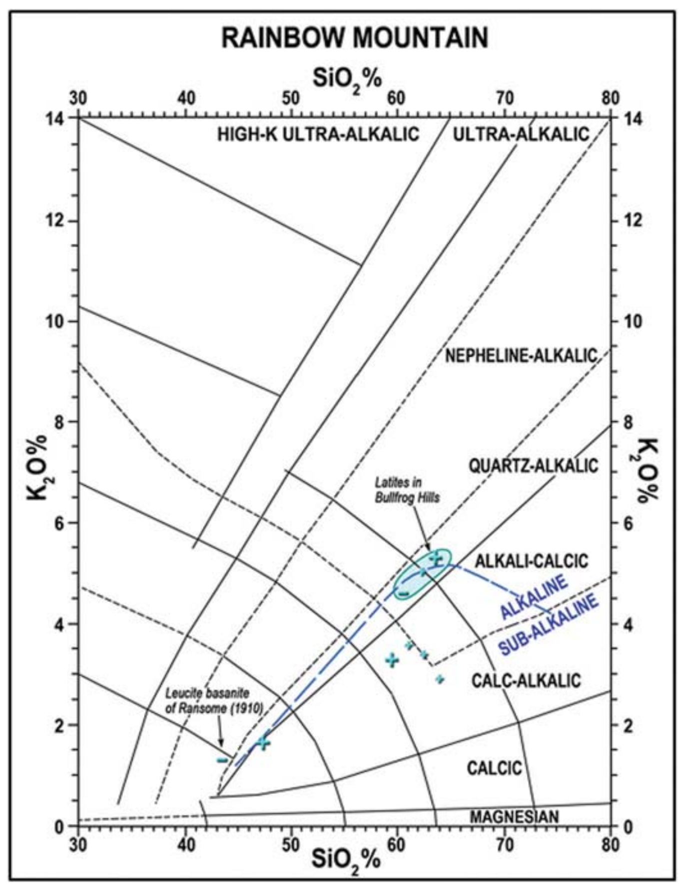

Figure 6. K_2O versus SiO_2 variation diagram for Rainbow Mountain sequence indicating Quartz Alkalic magma-metal series model.

Barrick-Bullfrog mine near Rhyolite, Montgomery-Shoshone mine, and Original Bullfrog mine. These deposits are assigned to the MQA35 model.

Many of these localities are well constrained by K-Ar dates of various types on adularia. In the Bullfrog Hills, the mineral systems become younger from the northeast to the southwest. The Mayflower-Pioneer has yielded K-Ar adularia ages ranging from 11.3 to 10±0.3 Ma (Eng and others, 1996). To the southwest, the Rhyolite district containing the Barrick-Bullfrog mine yielded K-Ar adularia ages ranging from 9.99 to 10.07 Ma. In the western Bullfrog Hills, K-Ar ages range from 8.7 to 9.2 Ma on adularia at the Original Bullfrog mine.

Terminal Arc, Nepheline Alkalic Magmatism (MNA)

Ransome (1910) reported detailed descriptions and chemical analyses for a leucite basanite containing augite, olivine, leucite, magnetite, ilmenite, plagioclase, nepheline, biotite, apatite, and zircon. Chemical data for one sample of the leucite biotite basanite plots in the nepheline alkaline basalt field on a K_2O-SiO_2 variation diagram (Figure 7).

The biotite content of the leucite basanite suggests that it is related to the arc magmatic event rather than the comparatively anhydrous magmatism that appeared in the Crater Flat region after about 5 Ma. No significant amounts of hydrous ferromagnesian minerals have been reported from the post 5-Ma basalts (Crowe and others, 1995; Heizler and others, 1999).

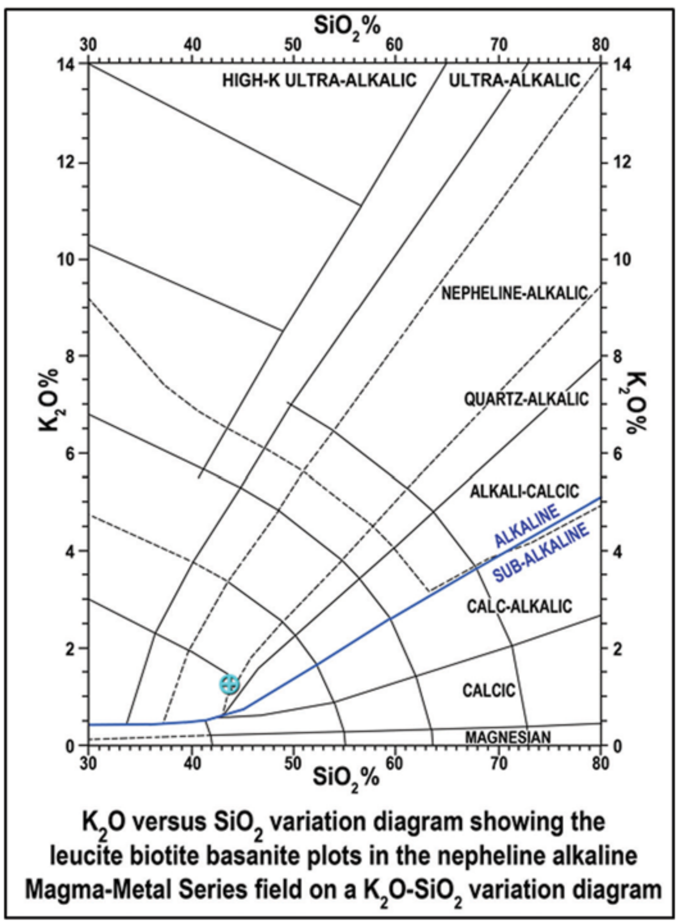

Figure 7. K_2O versus SiO_2 variation diagram of the leucite biotite basanite showing Metaluminous Nepheline Alkalic (MNA) magma-metal series.

The leucite basanite was only identified at three localities: on the flat to the southwest of the summit of Rainbow Mountain (where the sample for chemical analysis was collected), on the flat to the north of Montgomery Mountain, and on the south slope of the hill (elevation 3,580 feet) about 4,000 feet south of Beatty (Ransome, 1910). The nepheline alkaline (MNA) petrography and chemistry are consistent with mafic, quartz-deficient intrusions associated with gold deposits in other MNA46 and MNA47 models. The presence of olivine-magnetite-ilmenite indicates low oxidation and the occurrence of biotite indicates hydrous crystallization conditions.

Late Stage, Au-Te-Th-F-LREE Mineralization (MNA46)

Geochemical anomalies consist of molybdenum, cerium, lanthanum, barium, strontium, and uranium and slightly elevated tellurium, thallium, arsenic, tungsten, thorium, zinc, and mercury. These are characteristic of the gold-telluride systems of model MNA46. At the Life Preserver mine in the Tolicha district, highly anomalous thorium, light rare earth elements, strontium, and barium are intimately associated with the gold occurrence. In the Secret Pass/Daisy deposits, gold-copper metallization is associated with widespread fluorite. Many of these elements are highly anomalous in sample numbers YMR 0879 and YMR 0850 (Castor and others, 1999).

At the Oasis Mountain mine, Castor and others (1999) reported that gold was being or has been produced from telluride ores. The Oasis Mountain Project (Spicer Claim) north of Beatty, near Springdale, was producing telluride gold ore for over a year, and the district had been extensively explored for precious metals during 1981–1982 (Castor and others, 1999). Because of their highly economic pedigrees, gold occurrences that contain nepheline alkalic signatures are worth further investigation.

Subduction-related magmatism ended in the Yucca Mountain region around 6 Ma. The Spearhead member of the Thirsty Canyon Tuff erupted from the Black Mountain caldera as the last major ash-flow sheet.

PLIOCENE-QUATERNARY BASALTIC MAGMATISM

Basaltic volcanism after 5 Ma is associated with a north-south zone called the Crater Flat volcanic zone (Crowe and others, 1995). Anhydrous, iron-rich, basaltic magmatism began about 4.88 Ma at several centers near Thirsty Mesa, where basalt was deposited on Thirsty Canyon Tuff. At the south end of the zone, basaltic magmatism started at about 3.7 Ma as the basalt of Amargosa Valley (Crowe and others, 1995). From north to south, Makani Cone, Red Cone and Black Cone (1.07–1.17 Ma) and Little Cones (0.78–0.99 Ma) were erupted starting at 1.17 Ma (Valentine and others, 2006).

Several types of basaltic volcanic rocks are present in Crater Flat (Vaniman and others, 1982; Bradshaw and Smith, 1994). The oldest volcanic rocks of cycle 1, which initiated between 4.8 and 3.7 Ma, are mostly quartz normative basalts, with a minor hypersthene component and lower LREE and strontium compared to the younger basaltic volcanism. The next younger cycle of volcanic rocks (circa 1.1 Ma) in Crater Flat are hypersthene normative and contain lesser amounts of Ce, La, Ba, and Sr compared to the younger volcanism (circa 0.85 Ma at Little Cones), which is nepheline normative.

These three types of basalt come from three broad layers of the layered earth model (Figure 8). The quartz-normative magmatism represents basaltic partial melts extracted from an eclogitic upper asthenosphere, which is the source of MCA and MAC magmas. The quartz-deficient, hypersthene-normative basalts represent magmas extracted from the high-aluminum spinel lherzolite, which is the source of MQA magmas. The youngest MNA nepheline normative basalts represent magmas extracted from the chrome-rich spinel lherzolites in the lower asthenosphere. Regionally, alkalinity increases with decreasing age in any given volcanic center (Annis and Keith, 1986). Thus, in younger parts of the volcanic system, the cone of adiabatic decompression extends into deeper parts of the asthenosphere, where it taps increasingly silica-deficient nepheline alkaline source areas.

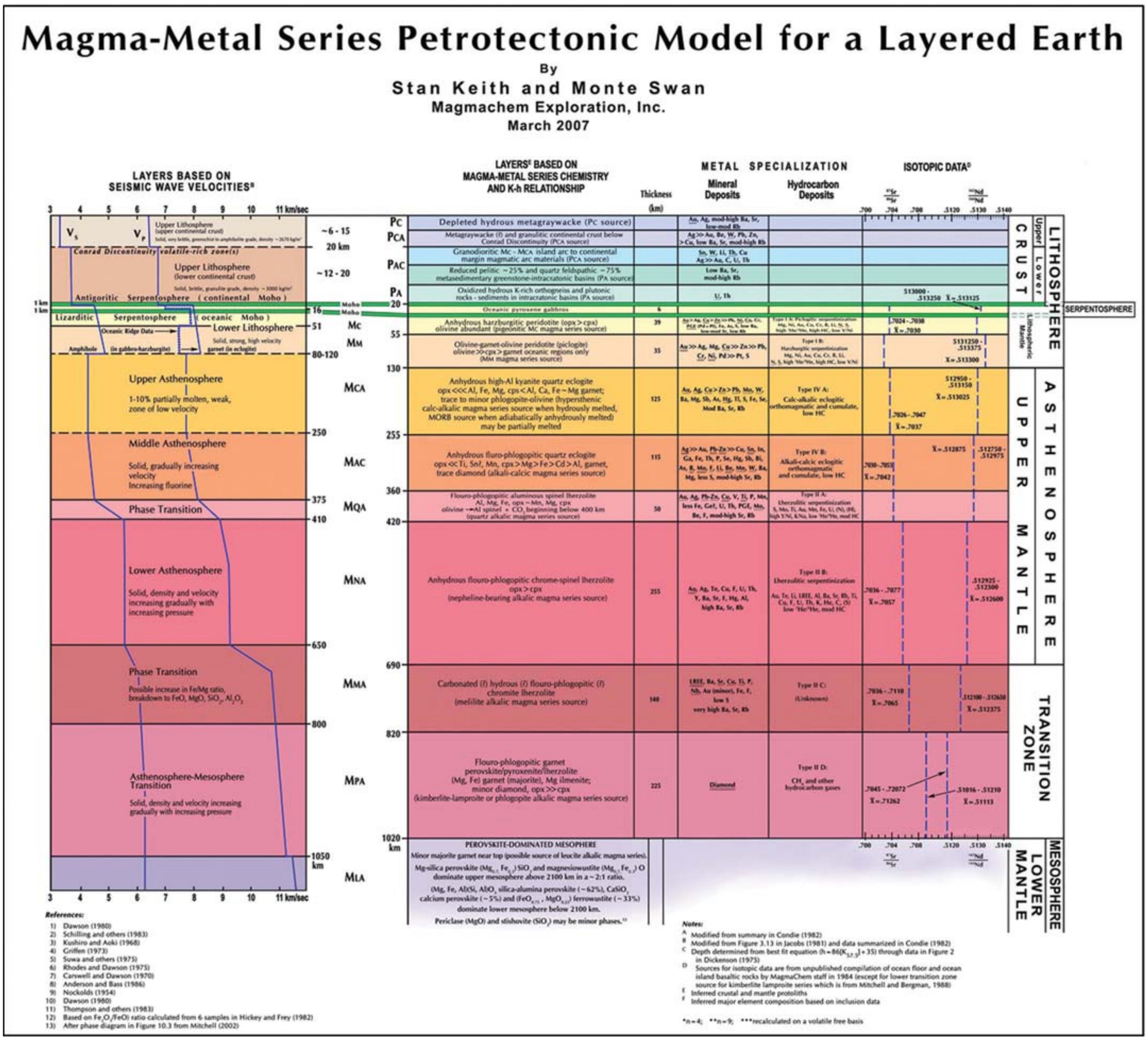

Figure 8. Magma-metal series petrotectonic model for a layered Earth.

In southwestern Nevada, modern basaltic activity has followed active Basin and Range faulting and has shifted to the west into Death Valley, Owens Valley, and Panamint Valley. Examples include active volcanic fields at Little Lake and Lone Pine, California, in the Owens Valley, and the Ubehebe crater in northern Death Valley.

TERTIARY-QUATERNARY UDH HYDROTHERMAL HYDROCARBONS?

Hydrothermal activity shown by the presence of Late Tertiary to Quaternary basalts and magnesium metasomatism allow the possibility that Ultra-Deep Hydrocarbon (UDH) processes could have been operating at Crater Flat. Coinciding magnetic highs and gravity lows, which occur in Crater Flat near Red Cone (O'Leary, 2007), are a common characteristic of UDH petroleum (Figure 9).

Evidence supporting a possible UDH system at Crater Flat includes extensive dolomitization in Paleozoic rocks, the presence of radiogenic strontium, and widespread magnesian calcite formed between 2 to 0 Ma (data from Wilson and others, 2003). Neymark and others (2000, 2002) reported that lukewarm, near-ambient temperature fluids used an older fracture net that dendritically forked upward; that is consistent with upwelling fluids. These fluids could represent low temperature, magnesium- and carbonate-charged fluids that emanated from a deep UDH source. Such fluids would have produced magnesian calcite seeps at or near the ground surface and in shallow fracture systems, such as illustrated by Menges and others (2000).

A possible serpentinite diapir and associated UDH system could have used normal faults on the east side of the Crater Flat graben, shown in O'Leary (2007), Stuckless and O'Leary (2007), and Valentine and others (2006). The main elements of the magnetic high are associated with north-south, tensional jogs on NNE-trending faults. The north-south jog on the Crater Flat fault could have been a route for rising magnesium-charged brines that were related to the possible serpentine diapirs.

Oil shales consistent with UDH activity occur in Area 8 in the NE portion of the Nevada Test Site (Figure 1), as reported in a petroleum source rock evaluation by Barker (1995). In Area 8, several carbonaceous shales contained total "organic" carbon (TOC) values between 6.14% and 26.43% hydrocarbon (kerogen reported as TOC) (Barker, 1995; French, 1997). These carbonaceous sediments could be interpreted as chemical "mud" produced during mud "volcanism" at the top of a possible mud volcano. This Area 8 system is probably separate from the Crater Flat UDH system to the southwest (Figure 1), and is approximately halfway between Crater Flat and the Railroad Valley UDH hydrothermal hydrocarbon system to the northeast described by Hulen and others (1994).

French (1997) suggested that the best site for possible hydrocarbon occurrences was at Crater Flat. This conclusion coincides with the site predicted by the UDH hydrothermal hydrocarbon model. French considered Railroad Valley to be an analog for Crater Flat. Railroad Valley exhibits evidence of hydrothermal oil occurrences, and is similar to those at Bacon Flat and Grant Canyon (Hulen and others, 1994). The lack of oil seeps in Crater Flat is not evidence for lack of an oil system, as oil seeps were not in evidence when Railroad Valley was discovered. The best place to find the oil portion of the UDH system would be under Crater Flat, where it may be associated with reservoirs hosted in hydrothermal dolomite.

QUATERNARY CALCRETE AND PEDOGENIC DEPOSITS

At Yucca Mountain, there is no evidence that Basin and Range faults have experienced movement for the last 10,000 years (Taylor and Huckins, 1995). The youngest colluvial deposits have well-developed caliche soils developed above them and were deposited unconformably across the faults. Quaternary calcrete deposits demonstrate the lack of recent tectonism. Slope or bedded calcretes were formed by calcium carbonate leaching and redeposition in C-horizon caliche zones. The lower unit, which yielded dates of 488,000 to 270,000 years, is mineralized with silica and probable magnesium-enriched calcite. These calcrete deposits are analogous to the opal and magnesian calcite overgrown on older minerals in the Exploratory Studies Facility. These minerals yielded uranium-lead dates as young as 329,000 to 275,000 years (Wilson and others, 2003). The low temperature hydrothermal seep system appears to have gone extinct after about 200,000 years. As such, the seep system on the Bow Ridge fault could be related to the distal edges of the possible UDH system beneath Crater Flat. Stability of faults and lack of volcanism and associated hydrothermal activity during the Holocene were important regulatory considerations in the integrity and quality assurance of the proposed Yucca Mountain repository, required to last several tens of millennia.

SUMMARY AND CONCLUSIONS

Magma-metal series models were used to characterize mineralization at Yucca Mountain and nearby areas in southwestern Nevada. The assessment was updated with models related to the ultra-deep hydrocarbon (UDH) model, which suggests that oil can be formed hydrothermally via deep-sourced serpentinization processes.

Cretaceous mineralization in the area began with MAC29B lead-zinc-silver deposits at 102–99 Ma and later MCA14 porphyry copper-molybdenum geochemistry at 93–96 Ma. These were followed by PC2 tungsten in pegmatite dikes of Late Cretaceous age and then by PCA3A gold-quartz veins at 85–72 Ma. This pattern resulted from flattening subduction.

Tertiary mineralization includes: MCA gold mineralization at 13.8–14.9 Ma; MAC base-metal tin or fluoride mineralization at 12.8–11.2 Ma; MQA gold mineralization at 10 Ma; and MNA gold-telluride mineralization at 8 Ma. The increasing al-

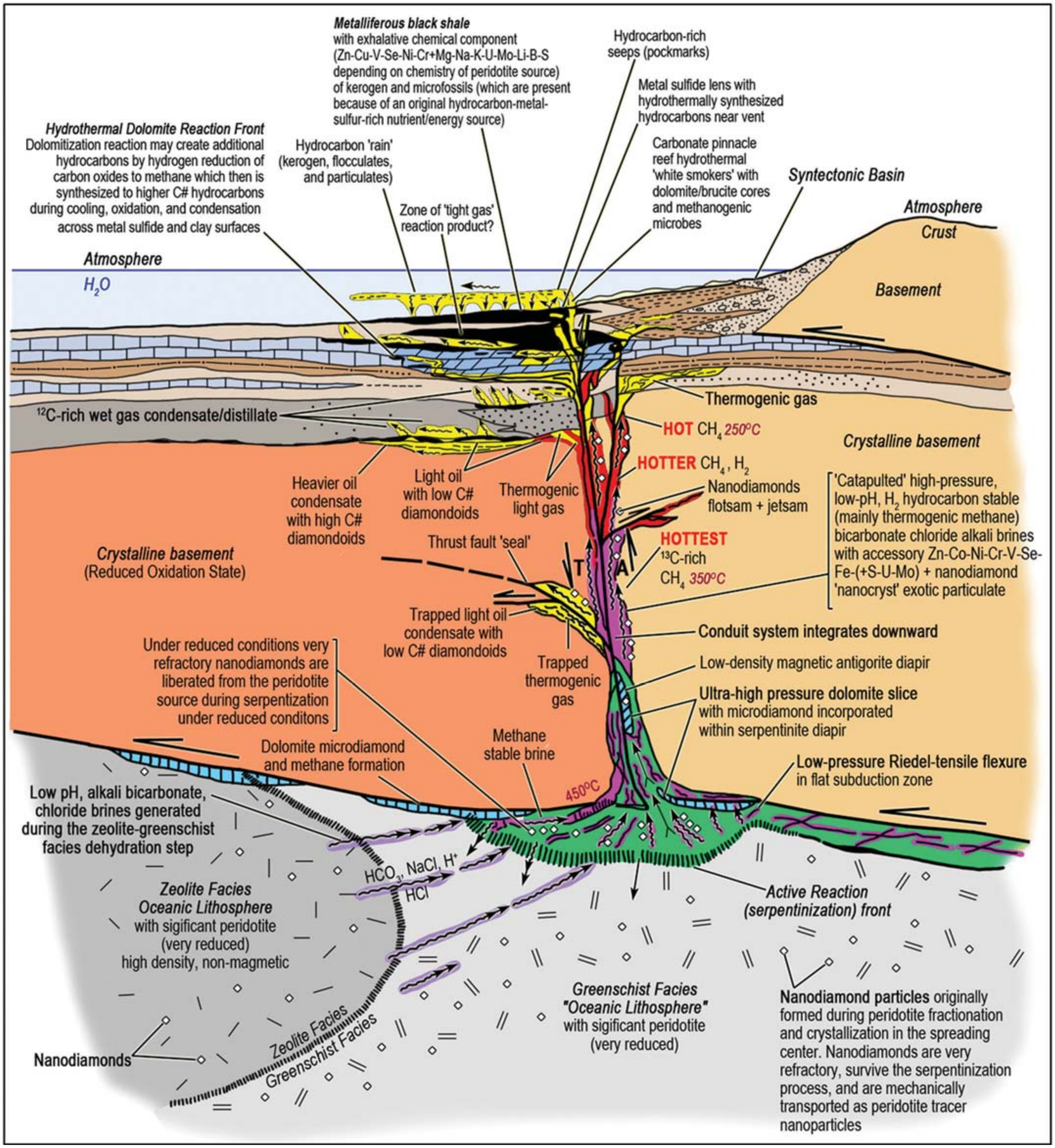

Figure 9. Conceptual UDH model showing how hydrothermal petroleum results from the serpentinization process in flat subduction settings (redrawn from Keith and Swan, 2005). (See Figure 3 for an updated model that includes the serpentosphere and supercritical/subcritical boundary.)

kalinity with decreasing age reflects a rapidly steepening subducting slab beneath the Yucca Mountain area between 15 and 7 Ma.

Magmatism after 7 Ma in the region is not associated with metallic mineralization and occurs as anhydrous, basaltic volcanic cones in Crater Flat. Modern basaltic activity has followed active Basin and Range faulting and has shifted to the west into Death Valley, Owens Valley, and Panamint Valley.

Hydrothermal activity after 7 Ma could be associated with a possible ultra-deep hydrocarbon (UDH) model. Evidence for a Pliocene-Quaternary hydrothermal event includes coincident gravity lows and magnetic highs in Crater Flat, widespread magnesian calcite and low-temperature hydrothermal activity, and comparisons with features at Railroad Valley.

Magmatism in the Southwest Nevada Volcanic Field probably did not access enough water during early fractionation to develop sufficient volume or chemical characteristics for a highly metal-rich hydrothermal fluid. Dry magmatism (lack of biotite and hornblende) is not associated with large, high-grade metal systems throughout the world. Certain volcanic units are slightly more water-rich and more voluminous than others and are associated with tin mineralization and alteration events. None of the multiple hydrothermal metallic mineralization events at Yucca Mountain itself are younger than approximately 11.4 Ma.

The potential for the existence, exploration, or discovery of economic metallic resources at the Yucca Mountain site is negligible for most commodities. Current markets and those in the foreseeable future are not likely to attract exploration companies to American tin occurrences. Potential for Carlin-type gold deposits may exist below approximately 5,000 feet in Paleozoic sedimentary rocks. However, nearby regions contain much higher potential for discovery of this type of gold deposits in the foreseeable future. Low potential exists for the discovery of mercury deposits. Potential for other metallic commodities, such as silver, copper, molybdenum, lead, zinc, iron, tungsten, antimony, and manganese, is negligible. There is , however, considerable potential for discovery of additional gold mineralization around the Beatty, Bullfrog and Bare Mountain areas, southwest of Yucca Mountain. The Nellis AFB Range, Nevada Test Site, and Yucca Mountain site are presently restricted from mineral entry and this is not likely to change in the foreseeable future.

ACKNOWLEDGEMENTS

We gratefully acknowledge the extensive work by numerous researchers who have thoroughly examined the rocks of the Nevada Test Site and Yucca Mountain through the support of the U.S. Department of Energy. This summary was based on previously published data, interpreted in a new way, using a synergistic approach to magmatism, mineralization, and tectonics. Woodward-Clyde Federal Services employed the principal author, and the second author was employed as a consultant for Chapter 6 of the Natural Resources Final Report of the Yucca Mountain area (CRWMS, 1997). Since that time, additional published information has been consulted. Research into the Ultra Deep Hydrocarbon (UDH) process during the last 15 years provided details on the hydrothermal oil potential. Research into hydrothermal oil in rift and flat subduction settings has been supported by several oil companies. The authors are especially grateful to Peg O'Malley for preparation of the illustrations.

REFERENCES CITED

Annis, D.R., and Keith, S.B., 1986, Petrochemical variation in post-Laramide igneous rocks in Arizona and adjacent regions: geotectonic and metallogenic implications, *in* Beatty, B., and Wilkinson, P.A.K., eds., Frontiers in Geology and Ore Deposits of Arizona and the Southwest: Arizona Geological Society Digest, v. 16, p. 448–456.

Armstrong, R.L., 1972, Low-angle (denudation) faults, hinterland of the Sevier orogenic belt, eastern Nevada and western Utah: Geological Society of America Bulletin, v. 83, p. 1729–1754.

Barker, C.E., 1995, Thermal and petroleum-generation history of the Mississippian Eleana Formation and Tertiary source rocks, Yucca Mountain area, southern Nye County, Nevada: American Association of Petroleum Geologists, v. 79, no. 6, June, Conf-9507131, Rocky Mountain Section meeting, Reno, NV, July 16-19, no pagination.

Barr, D.L., Moyer, T.C., Singleton, W.L., Albin, A.L., Lung, R.C., Lee, A.C., Beason, S.C., and Eatman, G.L.W., 1996, Geology of the North Ramp—stations 4+00 to 28+00, exploratory studies facility, Yucca Mountain Project, Yucca Mountain, Nevada: U.S. Bureau of Reclamation and U.S. Geological Survey report for Nevada Operations Office, U.S. Department of Energy, 179 p.

Bradshaw, T.K., and Smith, E.I., 1994,Polygenetic Quaternary volcanism at Crater Flat, Nevada: Journal of Volcanology and Geothermal Research, v. 63, no. 3–4, p. 165–182.

Brocher, T.M., and Hunter, W.C., 1996, Seismic reflection evidence against a shallow detachment beneath Yucca Mountain, Nevada: High-Level Radioactive Waste Management Proceedings of the Seventh International Conference, Las Vegas, Nevada, p. 148–150.

Brocher, T.M., Hart, P.E., Hunter, W.C., and Langenheim, V.E., 1996, Hybrid-source seismic reflection profiling across Yucca Mountain, Nevada; regional Lines 2 and 3: U.S Geological Survey Open-File Report 96–28, 111 p., 8 plates.

Brocher, T.M., Hunter, W.C., and Langenheim, V.E., 1998, Implications of seismic reflection and potential field geophysical data on the structural framework of the Yucca Mountain-Crater Flag region, Nevada: Geological Society of America Bulletin, v. 110, p. 947–971.

Broxton, D.E., Warren, R.G., Hagan, R.C., and Luedemann, G., 1986, Chemistry of diagenetically altered tuffs at a potential nuclear waste repository, Yucca Mountain, Nye County, Nevada: Los Alamos National Laboratory, LA-10802-MS, UC-70, 160 p.

Broxton, D.E., Warren, R.G., Byers, F.M., and Scott, R.B., 1989, Chemical and mineralogic trends within the Timber Mountain-Oasis Valley caldera complex, Nevada: evidence for multiple cycles of chemical evolution in a long-lived silicic magma system: Journal of Geophysical Research, v. 94, no. B5, p. 5961–5985.

Carr, W.J., 1990, Styles of extension in the Nevada Test Site region, southern Walker Lane belt: An integration of volcano-tectonic and detachment fault models, *in* Wernicke, B. P., ed., Basin and Range extensional tectonics near the latitude of Las Vegas, Nevada: GSA Memoir 176, p. 283–303.

Caskey, S.J., and Schweickert, R.A., 1992, Mesozoic deformation in the Nevada Test Site and vicinity: implications for the structural framework of the Cordilleran fold and thrust belt and Tertiary extension north of Las Vegas Valley: Tectonics, v. 11, p. 1314–1331.

Castor, S.B., Garside, L.J., Tingley, J.V., LaPointe, D.D., Desilets, M.O., Hsu, L.-C., Goldstrand, P.M., Lugaski, T.P., and Ross, H.P., 1999, Assessment of metallic mineral resources in the Yucca Mountain conceptual controlled area, Nye County, Nevada: Nevada Bureau of Mines and Geology, Reno, NV, Open-File Report 99-13, 204 p. plus appendices and plates.

Crowe, B., Perry, F., Geissman, J., McFadden, L., Wells, S., Murrell, M., Poths, J., Valentine, G.A., Bowker, L., and Finnegan, K., 1995, Status of volcanism studies for the Yucca Mountain Site Characterization Project: Los Alamos National Laboratory, LA-12908-MS, UC-802, 399 p.

CRWMS, 1997, Natural Resources Final Report, Yucca Mountain Area, Nye County, Nevada: prepared by Civilian Radioactive Waste Management System Management & Operating Contractor for Department of Energy, Yucca Mountain Site Characterization Office, Deliverable No. SP23GM3, Document Identifier # B00000000-01717-5700-00005, Chapters 2 (67 p.), 5 (125 p. plus appendices and figures), 6 (79 p. plus appendices and figures), and 7 (113 p.).

Eng, T., Boden, D.R., Reischman, M.R., Biggs, J.O 1996, Geology and mineralization of the Bullfrog Mine and vicinity, Nye County, Nevada, *in* Coyner, A.R., and Fahey, P.L., eds., Geology and Ore Deposits of the American Cordillera, Symposium proceedings, Geological Society of Nevada, v. 1, p. 353–402.

Farmer, G.L., Broxton, D.E., Warren, R.G., and Pickthorn, W., 1991, Nd, Sr, and O isotopic variations in metaluminous ash-flow tuffs and related volcanic rocks at the Timber Mountain/Oasis Valley caldera, complex, SW Nevada: implications for the origin and evolution of large-volume silicic magma bodies: Contributions to Mineralogy and Petrology, v. 109, p. 53–68.

Feighner, M., Johnson, L., Lee, K., Daley, T., Karageorgi, E., Parker, P., Smith, T., Williams, K., Romero, A., and McEvilly, T., 1996, Results and interpretation of multiple geophysical surveys at Yucca Mountain, Nevada: Lawrence Berkeley National Laboratory LBL-38200, 139 p.

Fleck, R.J., Lanphere, M.A., Turrin, B., and Sawyer, D.A., 1991, Chronology of late Miocene to Quaternary volcanism and tectonism in the southwest Nevada volcanic field (abs.): Geological Society of America Abstracts with Programs, v. 23, p. 25.

Flood, T.P., Vogel, T.A., and Schuraytz, B.C., 1989, Chemical evolution of a magmatic system: the Paintbrush Tuff, southwest Nevada volcanic field: Journal of Geophysical Research, v. 94, no. B5, p. 5943–5960.

French, Don E., 1997, Assessment of the potential for hydrocarbon in the Yucca Mountain area, Chapter 7, Hydrocarbon resources, in CRWMS, 1997, Natural Resources Final Report, Yucca Mountain Area, Nye County, Nevada: prepared by Civilian Radioactive Waste Management System Management & Operating Contractor for Department of Energy, Yucca Mountain Site Characterization Office, Deliverable No. SP23GM3, Document Identifier # B00000000-01717-5700-00005, Chapter 7, 113 p.

Fruh-Green, G.L., Connolly, J.A.D., and Plas, A., 2004, Serpentinization of oceanic peridotites: implications for geochemical cycles and biological activity, in The Subseafloor Biosphere at Mid-Ocean Ridges: American Geophysical Union, Geophysical Monograph Series 144, p. 119–136.

Hazen, R.M., Hemley, R.J., Mangum, A.J., 2012, Carbon in Earth's interior: storage, cycling, and life: Eos: Transactions American Geophysical Union, v. 93, p. 17–28.

Heizler, M.T., Perry, F.V., Crowe, B.M., Peters, L., and Appelt, R., 1999, The age of Lathrop Wells volcanic center: an $^{40}Ar/^{39}Ar$ dating investigation: Journal of Geophysical Research, v. 104, no. B1, p. 767–804.

Hoisch, T.S., and Simpson, C., 1993, Rise and tilt of metamorphic rocks in the lower plate of a detachment fault in the Funeral Mountains, Death Valley, California: Journal of Geophysical Research, v. 98, p. 6805–6827.

Houser, F.N., and Poole, F.G., 1960, Preliminary geologic map of the Climax stock and vicinity, Nye County, Nevada: U.S. Geologic Survey map I-328, 2 sheets, scale 1:48,000.

Hulen, J.B., Goff, F., Ross, J.R., Bortz, L.C., and Bereskin, S.R., 1994, Geology and geothermal origin of Grant Canyon and Bacon Flat oil fields, Railroad Valley, Nevada: American Association of Petroleum Geologists Bulletin, v. 78, no. 4, p 596–623.

Jackson, M.R.. Jr., 1988, The Timber Mountain magmato-thermal event: an intense widespread culmination of magmatic an hydrothermal activity at the southwestern Nevada volcanic field: University of Nevada, Reno–Mackay School of Mines, Reno, Nevada, M.S thesis, 46 p.

Johnston, K., Keith, S., Johnston, P., and Swan, M., 2010, Origin of the Green River kerogen by serpentinite-powered hydrothermalism: AAPG Search and Discovery Article #90108©2010 AAPG International Convention and Exhibition, September 12–15, 2010 Calgary, Alberta, Canada, 2 p.

Jones, C.H., Mahan, K.H., Butcher, L.A., Levandowski, W.B., and Farmer, G.L., 2015, Continental uplift through crustal hydration: Geology, April 2015, doi:10.1130/G36509.1, GSA Data Repository item 2015128.

Keith, S.B., 1986, Petrochemical variations in Laramide magmatism and their relationship to Laramide tectonic and metallogenic evolution in Arizona and adjacent regions: Arizona Geological Society Digest, v. 16, p. 89–101.

Keith, S.B., 2002, Magma-metal series Appendix II: Model table, classification chart, and explanatory text: Private report distributed to numerous clients, Table 5, 167 p.

Keith, S.B., and Swan, M.M., 1996, The great Laramide porphyry copper cluster of Arizona, Sonora, and New Mexico: the tectonic setting, petrology, and genesis of a world class porphyry metal cluster, *in* Coyner, A. R., and Fahey, P. L., eds., Geology and ore deposits of the American Cordillera, Symposium Proceedings: Geological Society of Nevada, v. III, p. 1667–1747.

Keith, S.B., and Swan, M.M., 2005, Hydrothermal hydrocarbons (abs.): Goldschmidt Conference abstracts: accessed at http://www.searchanddiscovery.com/documents/abstracts/2005research_calgary/abstracts/extended/keith/keith.htm 4/

Keith, S.B., and Swan, M.M., 2010, On the origin of kerogen: June 13–18, 2010, Goldschmidt 2010 Earth, Energy, and Environment, Knoxville, TN. http://www.searchanddiscovery.com/documents/abstracts/2005research_calgary/abstracts/extended/keith/keith.htm

Keith, S.B., and Wilt, J.C., 1985, Late Cretaceous and Cenozoic orogenesis of Arizona and adjacent regions; a stratotectonic approach, *in* Flores, R. M., Kaplan, S. S., eds., Cenozoic paleogeography of the west-central United States: Society of Economic Paleontologists and Mineralogists, Rocky Mountain Section, p. 403–437.

Keith, S.B., and Wilt, J.C., 1986, Laramide Orogeny in Arizona and adjacent regions; a stratotectonic synthesis, *in* Beatty, B., and Wilkinson, P.A.K., eds., Frontiers in geology and ore deposits of Arizona and the southwest: Tucson, Arizona Geological Society Digest, v. 16, p. 502–554.

Keith, S.B., Laux, D.P., Maughan, J., Schwab, K., Ruff, S., Swan, M.M., Abbott, E., and Friberg, S., 1991, Magma series and metallogeny: a case study from Nevada and environs, *in* Buffa, Ruth H., and Coyner, Alan R., editors, Geology and ore deposits of the Great Basin; field trip guidebook compendium: Geologic Society of Nevada, Reno, NV, p. 404–493.

Keith, S.B., Swan, M., Rueslatten, H., Johnsen, H.K., and Page, N., 2008, The serpentosphere: Geological Society of Nevada newsletter, v. 23, no. 3, p. 3.

Levy, S. S., Norman, D. I., and Chipera, S. J., 1996, Alteration history studies in the Exploratory Studies Facility, Yucca Mountain, Nevada, USA: Material Research Society Symposium Proceedings, v. 412, p. 783–790.

Lewan, M.D., 1997, Experiments on the role of water in petroleum formation: Geochimica et Cosmochimica Acta, v. 61, no. 17, p. 3691–3723.

Lipman, P. W., Christiansen, R. L., and O'Connor, J. T., 1966, A compositional zoned ash-flow sheet in southern Nevada: U.S. Geologic Survey Professional Paper 524-F, 47 p.

Maldonado, F., 1977, Summary of the geology and physical properties of the Climax Stock, Nevada Test Site: U.S. Geological Survey Open-File Report 77356.

Maldonado, F., 1981, Geology of the Twinridge pluton area, Nevada Test Site, Nevada: U. S. Geological Survey Open-File Report 81-156, 33 p.

Marvin, R.F., Byers, F.M., Jr., Mehnert, H.H., Orkild, P.P., and Stern, T.W., 1970, Radiometric ages and stratigraphic sequence of volcanic and plutonic rocks, southern Nye and western Lincoln Counties, Nevada: Geological Society of America Bulletin v. 81, p. 2657–2676.

Marvin, R.F., Mehnert, H.H., and Naeser, C.W., 1989, U.S. Geological Survey radiometric ages—compilation "C", part 3: California and Nevada: Isochron/West, no. 52, p. 3–11.

Mattson, S., Clayton, R.W., Ely, R.W., Wilt, J.C., Nelson, S.T., Castellanous, M., and Matthusen, A.C., 1994, Yucca Mountain Project draft stratigraphic compendium: U.S. Department of Energy, Contract De-ac01-91w00134, 154 p.

Menges, C.M., Cress. R., Vadurro, G., Simonds, F.W., Coe, J.A., and Murray, M., 2000, Logs and paleoseismic interpretations from trenches 14C and 14D on the Bow Ridge Fault, Nevada: U.S. Geological Survey Miscellaneous Field Studies Map MF-2311, 4 plates of cross sections at various scales.

Monsen, S. A., Carr, M. D., Reheis, M. C., and Orkild, P. P., 1990, Geologic map of Bare Mountain, Nye County, Nevada: U.S. Geological Survey Open-File Report 90-25, 21 p., scale 1:24,000.

Monsen, S. A., Carr, M. D., Reheis, M. C., and Orkild, P. P., 1992, Geologic map of Bare Mountain, Nye County, Nevada: U.S. Geological Survey Miscellaneous Investigations Map I-2201, scale 1:24,000.

Naeser, C. W., and Maldonado, Florian, 1981, Fission-track dating of the Climax and Gold Meadows stocks, Nye County, Nevada: U.S. Geological Survey Professional Paper 1199-E, p. 45–46.

Neymark, L.A., and Paces, J.B., 2000, Consequences of slow growth for ^{230}Th/U dating of Quaternary opals, Yucca Mountain, NV, USA: Chemical Geology, v. 164, p. 143–160.

Neymark, L.A., Amelin, Y., Paces, J.B., and Peterman, Z.E., 2002, U-Pb ages of secondary silica at Yucca Mountain, Nevada: Implications for the paleohydrology of the unsaturated zone: Applied Geochemistry, v. 17, p. 709–734.

Noble, D.C., Weiss, S. I., and McKee, E.H., 1991, Magmatic and hydrothermal activity, caldera geology, and regional extension in the western part of the southwestern Nevada volcanic field, *in* Raines, G.L., Lisle, R.E., Shafer, R.W., and Wilkinson, W.W., eds., Geology and ore deposits of the Great Basin: Symposium proceedings, Geological Society of Nevada , p. 913–934.

O'Leary, D.W., 2007, Tectonic models for Yucca Mountain, Nevada: Geological Society of America Memoir 199, p. 105–153.

Papike, J.J., Keith, T.E.C., Spilde, M.N., Galbreath, K.C., Shearer, C.K., and Laul, J.C., 1991, Geochemistry and mineralogy of fumarolic deposits, Valley of Ten Thousand Smokes, Alaska: Bulk chemical and mineralogical evolution of dacite-rich protolith: American Mineralogist, v. 76, p. 1,662–1,673.

Peterman, Z.E., Spengler, R.W., Singer, F.R., and Beason, S.C., 1996, Localized alteration of the Paintbrush nonwelded hydrologic unit within the Exploratory Studies Facility: Proceedings of the 7th annual conference on High-Level Radioactive Waste Management, v. 1, p. 46–47.

Quade, J., Tingley, J.V., Bentz, J.L., and Smith, P.L., 1984, A mineral inventory of the Nevada Test Site and portions of Nellis Bombing and Gunnery Range, southern Nye County, Nevada: Nevada Bureau of Mines and Geology Open-File Report 84-2, 40 p.

Ransome, F. L., 1910, Geology and ore deposits of the Goldfield district, Nevada: Economic Geology, v. 5, Part 1, p. 301–311, Part 2, p. 438-470.

Sawyer, D.A., Fleck, R.J., Lanphere, M.A., Warren, R.G., Broxton, D.E., and Hudson, M.R., 1994, Episodic caldera volcanism in the Miocene southwestern Nevada volcanic field: Revised stratigraphic framework, ^{40}Ar/^{39}Ar geochronology, and implications for magmatism and extension: Geological Society of America Bulletin, v. 106, p. 1304–1318.

Schuraytz, B.C., Vogel, T.A., and Younker, L.W., 1989, Evidence for dynamic withdrawal from a layered magma body: the Topopah Spring Tuff, southwestern Nevada: Journal of Geophysical Research, v. 94, no. B5, p. 5925–5942.

Scott, R.B., 1990, Tectonic setting of Yucca Mountain, southwest Nevada, *in* Wernicke, B.P., ed., Basin and Range extensional tectonics near the latitude of Las Vegas, Nevada: Boulder, Colorado, Geological Society of America Memoir 176, p. 251–282.

Simonds, F.W., 1989, Geology and hydrothermal alteration in the Calico Hills, southern Nevada: Fort Collins, Colorado, Colorado State University, M.S. thesis, 136 p.

Stewart, J.H., 1980, Geology of Nevada: Nevada Bureau of Mines and Geology Special Publication 4, 136 p.

Stewart, J.H., and Carlson, J.E., 1976, Cenozoic rocks of Nevada - Four maps and a brief description of distribution, lithology, age, and centers of volcanism: Nevada Bureau of Mines and Geology Map 52, scale 1:1,000,000.

Stuckless, J.S., and O'Leary, D.W., 2007, Geology of the Yucca Mountain region, *in* Stuckless, J.S., and Levich, R.A., eds., The geology and climatology of Yucca Mountain and vicinity, southern Nevada and California: Geological Society of America, Memoir 199, p. 9–52.

Taylor, E.M., and Huckins, H.E., 1995, Lithology, fault displacement, and origin of secondary calcium carbonate and opaline silica at Trenches 14 and 14D on the Bow Ridge fault at Exile Hill, Nye County, Nevada: U.S. Geological Survey Open-File Report 93-477, 34 p.

Tingley, J.V., Castor, S.B., Garside, L.J., Weiss, S.I., Bonham, H.F., Jr., La Pointe, D.D., Lugaski, T.P., Price, J.F., and Desilets, M., 1996, Mineral and energy resource assessment of the Nellis Air Force Range: Nevada Bureau of Mines and Geology draft report to the Nellis Air Force Base Environmental Management, and U. S. Army Corps of Engineers Fort Worth District Planning Division, Fort Worth, Texas, 738 p. plus appendices.

Tingley, J.V., Castor, S.B., Weiss, S.I., Garside, L.J., Price, J.G., LaPointe, D.D., Bonham, H.F., Jr., and Lugaski, T.P., 1998, Mineral and energy resource assessment of the Nellis Air Force Range, U.S. Air Force Air Combat Command, Clark, Lincoln, and Nye Counties, Nevada: Nevada Bureau of Mines and Geology, Open-File Report 98-01, v. 1 and 2, 735 p.

Valentine, G.A., Perry, F.V., Krier, D., Keating, G.N., Kelley, R.E., and Cogbill, A.H., 2006, Small-volume basaltic volcanoes: eruptive products and processes, and posteruptive geomorphic evolution in Crater Flat (Pleistocene), southern Nevada: Geological Society of America Bulletin, v. 118, no. 11/12, p. 1313–1330.

Vaniman, D.R., Crowe, B.M., and Gladney, E.S., 1982, Petrology and geochemistry of hawaiite lavas from Crater Flat, Nevada: Contributions to Mineralogy and Petrology, v. 80, p. 341–357.

Warren, R.G., Byers, F.M., Broxton, D.E., Freeman, S.H., and Hagan, R.C., 1989, Phenocryst abundances and glass and phenocryst compositions as indicators of magmatic environments of large-volume ash flow sheets in southwestern Nevada: Journal of Geophysical Research, v. 94, no. B5, p. 5987–6020.

Weiss, S.I., Noble, D.C., and Larson, L.T., 1995, Hydrothermal origin and significance of pyrite in ash-flow tuffs at Yucca Mountain, Nevada: Economic Geology, v. 90, p. 2081–2090.

Wilson, N.S.F., Cline, J.S., and Amelin, Y.V., 2003, Origin, timing, and temperature of secondary calcite-silica mineral formation at Yucca Mountain, Nevada: Geochimica et Cosmochimica Acta, v. 67, no. 6, p. 1145–1176.

Wilt, J.C., 1993, Geochemical patterns of hydrothermal mineral deposits associated with calcalkalic and alkalicalcic igneous rocks as evaluated with neural networks: Tucson, Arizona, The University of Arizona, Ph. D. dissertation, 721 p.

Wilt, J.C., 1995, Correspondence of alkalinity and ferric/ferrous ratios of igneous rocks associated with various types of porphyry copper deposits, *in* Pierce, F, and Bolm, J., eds., Bootprints along the Cordillera, porphyry copper deposits from Alaska to Chile: Arizona Geological Society Digest, v. 20, p. 180–200.

New Concepts *and* Discoveries

VOLUME II

EDITED BY

W. M. Pennell

L. J. Garside

CO-HOSTED BY

Geological Society of Nevada
Nevada Bureau of Mines and Geology
Society of Economic Geologists
United States Geological Survey

DEStech Publications, Inc.